UNIVERSIDADE DE SÃO PAULO
FACULDADE DE ODONTOLOGIA DE BAURU

RODRIGO FONSECA BUZO

Microscopic and immunohistochemical characterization of tumor development in immunocompromised mice xenografted with cancer stem cells of oral squamous cell carcinoma

Caracterização microscópica e imuno-histoquímica do desenvolvimento tumoral em camundongos imunodeficientes xenotransplantados com células-tronco de câncer de carcinoma epidermóide de boca

BAURU
2020

RODRIGO FONSECA BUZO

Microscopic and immunohistochemical characterization of tumor development in immunocompromised mice xenografted with cancer stem cells of oral squamous cell carcinoma

Caracterização microscópica e imuno-histoquímica do desenvolvimento tumoral em camundongos imunodeficientes xenotransplantados com células-tronco de câncer de carcinoma epidermóide de boca

Dissertação apresentada a Faculdade de Odontologia de Bauru da Universidade de São Paulo para obtenção do título de Mestre em Ciências no Programa de Ciências Odontológicas Aplicadas, na área de concentração Biologia Oral.

Orientadora: Prof.ª Dr.ª Camila de Oliveira Rodini Pegoraro

BAURU
2020

Buzo, Rodrigo Fonseca

Microscopic and immunohistochemical characterization of tumor development in immunocompromised mice xenografted with cancer stem cells of oral squamous cell carcinoma / Rodrigo Fonseca Buzo – Bauru, 2020.

79p. : il. ; 31cm.

Dissertação (Mestrado) – Faculdade de Odontologia de Bauru. Universidade de São Paulo

Orientador: Profa. Dra. Camila de Oliveira Rodini Pegoraro

Comitê de Ética da FOB/USP
CEEPA-Proc. Nº 002/2017
Data: 05/05/2017

FOLHA DE APROVAÇÃO

DEDICATÓRIA

*Primeiramente, a **Deus**, pela sua infinita graça, amor e misericórdia que me alcançam todos os dias, me encorajando a realizar este sonho.*

*Aos meus pais **Fred** e **Isabela**, que nunca mediram esforços para me ajudar a chegar até aqui. Amo vocês. Agradeço por sempre estarem ao meu lado.*

AGRADECIMENTOS ESPECIAIS

Em especial agradeço,

*A minha orientadora **Profa. Dra. Camila de Oliveira Rodini**, por me orientar na elaboração deste trabalho. Obrigado pela confiança que depositou em mim. Saiba que você colaborou de forma imensurável para meu amadurecimento profissional.*

*À **Nádia Ghinelli Amôr**, por ser essa amiga e confidente que esteve ao meu lado desde o início, me mostrando sempre o bom que a vida tem para oferecer. Sou muito grato pela paciência em me corrigir e tranquilidade em me ensinar. Para mim, você é um exemplo de amor à pesquisa.*

*Ao **Rafael Carneiro Ortiz**, pela sua amizade e por cooperar grandemente em meu crescimento científico. Sou imensamente grato por todo sua dedicação com este projeto.*

*À **Luciana Mieli Saito** e **Nathália Martins Lopes** pelo apoio e contribuição como grupo de pesquisa. Sou grato por nossa amizade e bom convívio.*

*Às técnicas do laboratório de Histologia, **Danielle Ceolim e Patrícia Germínio**, pela inestimável ajuda prestada neste trabalho. Obrigado por sempre estarem ao me lado, me dando suporte e impulso nos momentos de dificuldade, e também me proporcionando momentos de bom-humor ao lado de vocês.*

*Às demais alunas do departamento de Histologia, **Angélica Fonseca**, **Jéssica Melchiades**, **Paula Sanches** e **Suelen Paini** pela convivência maravilhosa que temos no laboratório. Agradeço a colaboração e amizade.*

*A todos os demais **professores e funcionários da FOB-USP**, por estarem sempre dispostos a ajudar.*

Rodrigo Fonseca Buzo

AGRADECIMENTOS INSTITUCIONAIS

Ao Prof. Dr. Vahan Agopyan, *digníssimo reitor da Universidade de São Paulo;*

Ao Prof. Dr. **Pedro Vitoriano de Oliveira,** *digníssimo Secretário Geral da Universidade de São Paulo;*

Ao Prof. Dr. Carlos Ferreira dos Santos, *digníssimo Diretor da Faculdade de Odontologia de Bauru da Universidade de São Paulo;*

Ao Prof. Dr. Guilherme dos Reis Pereira Janson, *digníssimo Vice-diretor da Faculdade de Odontologia de Bauru da Universidade de São Paulo;*

Ao Prof. Dr. José Henrique Rubo, *digníssimo Prefeito do Campus da Faculdade de Odontologia de Bauru da Universidade de São Paulo;*

À Prof. Dra. Izabel Regina Fischer Rubira Bullen, *digníssima Presidente da Pós-Graduação da Faculdade de Odontologia de Bauru da Universidade de São Paulo;*

À Coordenação de Aperfeiçoamento de Pessoal de Nível Superior, CAPES, *pela bolsa concedida no meu mestrado;*

À Fundação de Amparo à Pesquisa do Estado de São Paulo (FAPESP), *órgão de fomento deste trabalho (número de processo: 2013/07245-9).*

“ Todas as vitórias ocultam uma abdicação. ”

Simone de Beauvoir

RESUMO

Caracterização microscópica e imuno-histoquímica do desenvolvimento tumoral em camundongos imunodeficientes xenotransplantados com células-tronco de câncer de carcinoma epidermóide de boca

O carcinoma epidermóide de boca (CEB) é uma das neoplasias mais comuns da região de cabeça e pescoço, com sobrevida global inferior a 5 anos. O pior prognóstico da doença está associado à presença de metástases linfonodais, que tem participação de uma subpopulação de células-tronco presente nos tumores, conhecidas por células-tronco de câncer (CSC, do inglês *cancer stem cells*). Essa subpopulação sofre transição epitélio-mesenquimal (EMT, do inglês *epitelial-mesenchymal transition*), processo no qual as células epiteliais adquirem um fenótipo mesenquimal tornando-se migratórias e invasivas. CSC podem ser identificadas por meio de biomarcadores, sendo a proteína CD44 a mais utilizada em CEB. Vale ressaltar que na pesquisa do câncer bucal, os modelos animais têm sido amplamente utilizados como estratégia para entender a carcinogênese, bem como para testar novos agentes antineoplásicos e desenvolver novas abordagens terapêuticas. O objetivo deste estudo foi avaliar e comparar microscopicamente tumores murinos induzidos por xenotransplante de duas subpopulações de CSC, $CD44^{High}ESA^{High}$ (epitelial) e $CD44^{High}ESA^{Low}$ (mensenquimal), presentes em linhagens de CEB humano LUC4. Após isolamento por meio de citometria de fluxo (BD FACSAria™ Fusion), foi realizado o xenotransplante das duas subpopulações com $5x10^3$ células inoculadas na língua, em dois grupos com 12 camundongos machos NOD/SCID cada. Após 49 dias, os tumores formados foram medidos, coletados e submetidos ao processamento histotécnico para caracterização microscópica e imuno-histoquímica. A subpopulação $CD44^{High}ESA^{High}$ apresentou maior potencial tumorigênico, formando tumores (média da área: 4,22 mm²) em todos os animais inoculados. Em contrapartida, apenas seis animais (50%) xenotransplantados com células $CD44^{High}ESA^{Low}$ desenvolveram tumores microscopicamente visíveis (média da área: 0,20 mm²). Foram observadas alterações estruturais e celulares semelhantes ao CEB de humanos em ambos os grupos. Além disso, os animais do grupo $CD44^{High}ESA^{High}$ apresentaram maior perda de peso comparado ao grupo $CD44^{High}ESA^{Low}$ ($p= 0,0217$). A correlação de subpopulações de CSC com seus tumores correspondentes *in vivo* representa uma abordagem confiável para futuras pesquisas sobre câncer bucal, destacando o papel de diferentes fenótipos de CSC no desenvolvimento e progressão de CEB. Estudos adicionais devem ser realizados

nesse campo, por exemplo, para entender como eles respondem na terapêutica comumente usada e desenvolver técnicas para superar os mecanismos de resistência.

Palavras-chave: Carcinoma Epidermóide. Células-tronco Neoplásicas. Transição Epitelial-Mesenquimal. Modelo Animal.

ABSTRACT

Microscopic and immunohistochemical characterization of tumor development in immunocompromised mice xenografted with cancer stem cells of oral squamous cell carcinoma

Oral squamous cell carcinoma (OSCC) is one of the most common neoplasms of the head and neck region, with overall survival <5 years. The worst prognosis of the disease is lymph node metastasis associated with a subpopulation of stem cells in tumors, known as cancer stem cells (CSC). Studies have shown that this subpopulation undergoes epithelial to mesenchymal transition (EMT), a process which epithelial cells acquire a mesenchymal phenotype. In OSCC, CSC can be identified by biomarkers, CD44 transmembrane protein being the most *commonly* used. In oral cancer research, animal models have been widely used as a strategy to understand carcinogenesis as well as to test new antineoplastic agents and to develop new therapeutic approaches. We aimed to evaluate and compare microscopically murine tumors induced by CSC xenotransplantation. Two subpopulations $CD44^{High}ESA^{High}$ (epithelial) and $CD44^{High}ESA^{Low}$ (mensenchymal) were isolated from OSCC cell line LUC4 by flow cytometry (BD FACSAria ™ Fusion). Xenotransplantation was performed with $5x10^3$ cells injected in the tongue into two groups with twelve NOD/SCID mice each one. Forty-nine days post-injection, tumors were measured, collected and submitted to histotechnical processing for microscopic and immunohistochemical analyses. $CD44^{High}ESA^{High}$ cells showed great tumorigenic potential, being able to originate larger tumors in twelve animals (average tumor area: 4.22 mm²). In contrast, only six animals (50%) xenografted with $CD44^{high}ESA^{low}$ cells developed microscopically visible tumors (average tumor area: 0.20 mm²). Structural and cellular changes similar to the human OSCC were observed in both groups. In addition, animals xenografted with $CD44^{High}ESA^{High}$ cells showed greater weight loss compared to the $CD44^{High}ESA^{Low}$ group ($p = 0.0217$). The correlation of CSC subpopulations with their corresponding tumors *in vivo* represents a reliable approach for future research in oral cancer, highlighting the role of different CSC phenotypes in OSCC development and progression. Further studies should be conduct in this field, for example, in understanding how they respond in commonly used therapeutics and develop techniques to overcome their resistance mechanisms.

Keywords: Squamous Cell Carcinoma. Neoplastic Stem Cells. Epithelial-Mesenchymal Transition. Animal Model.

LIST OF FIGURES

DISSERTATION

ARTICLE

LIST OF ABREVIATIONS

OSCC	Oral Squamous Cell Carcinoma
ITF	Invasive Tumor Front
CSC	Cancer Stem Cells
OCT-4	Octamer-binding Transcription Factor 4
SOX-2	Sex Determing Region Y-box 2
SC	Stem Cells
NOD/SCID	Non-obese Diabetic/severe Combined immunodeficient
ALDH1	Aldehyde Dehydrogenase Enzyme 1
BMI1	B-lymphoma Moloney murine leukemia virus insertion 1
HNSCC	Head and Neck Squamous Cell Carcinoma
TSSC	Tongue Squamous Cell Carcinoma
DMBA	9, 10-dimethyl-1, 2-benzanthracene
4NQO	4-nitroquinoline 1-oxide
DNA	Deoxyribonucleic acid
CEB	From Portuguese "*Carcinoma epidermóide de boca*"
CD44	Principal cell surface receptor for hyaluronate

SUMMARY

1 INTRODUCTION

1 INTRODUCTION

1.1 Oral squamous cell carcinoma

Oral squamous cell carcinoma (OSCC) is one of the most common malignant neoplasms of the head and neck region. It involves inner mucosa of the lips, tongue, floor of mouth, gingiva, palate, and buccal mucosa. The major risk factors for OSCC include the frequent use of tobacco and alcohol, as well as papilloma virus infection, associated with genetic susceptibility (PETRICK; WYSS; BUTLER; CUMMINGS *et al.*, 2014). The prognostic factor with the most significant impact is the presence of metastasis in cervical lymph nodes, which occurs in 25 to 65% of the cases (HANNEN; VAN DER LAAK; MANNI; PAHLPLATZ *et al.*, 2001; JÄRVINEN; AUTIO; KILPINEN; SAARELA *et al.*, 2008; KALLURI; WEINBERG, 2009; KOSUNEN; PIRINEN; ROPPONEN; PUKKILA *et al.*, 2007; SZANISZLO; FENNEWALD; QIU; KANTARA *et al.*, 2014; VERED; YAROM; DAYAN, 2005)

OSCC is microscopically characterized by islets and cords of tumor epithelial cells with cellular atypia (nuclear hyperchromasia, pleomorphism, altered nuclear-*cytoplasmic* ratio, frequent and abnormal mitoses, dyskeratosis and keratin pearls) and architectural changes (loss of stratification and basement membrane). The tumors are graded into well-diferentiated areas that resemble closely to normal squamous epithelium, moderately-differentiated areas exhibiting usually less keratinization, and poorly-differentiated (or undifferentiated) areas with predominance of immature cells and minimal keratinization (WHO, 2005). In addition, perivascular, perimuscular and perineural invasion by OSCC cells is often present in the invasive tumor front (ITF) that corresponds to three to six cell layers or detached tumor cell groups at the advancing edge (PIFFKÒ; BÀNKFALVI; OFNER; BRYNE *et al.*, 1997).

1.2 Cancer stem cells

Two hypotheses currently predominate to explain how cancer develops. In the stochastic model (Fig. 1A), all tumor cells are proliferative and display unlimited tumor-initiating capacities (WACLAW; BOZIC; PITTMAN; HRUBAN *et al.*, 2015). In contrast, the cancer

stem cells (CSC) theory (Fig. 1B) suggests that only one subpopulation among all tumor cells is highly proliferative and initiate a new tumor growth (CLEVERS, 2011; KOREN; FUCHS, 2016; REYA; MORRISON; CLARKE; WEISSMAN, 2001). However, the tumor hierarchy is not a one-way route, but can be reversible, which differentiated cells can dedifferentiate and obtain stem-like properties under specific conditions, such as OCT-4, Nanog and SOX-2 overexpression (HERREROS-VILLANUEVA; ZHANG; KOENIG; ABEL *et al.*, 2013; MEACHAM; MORRISON, 2013).

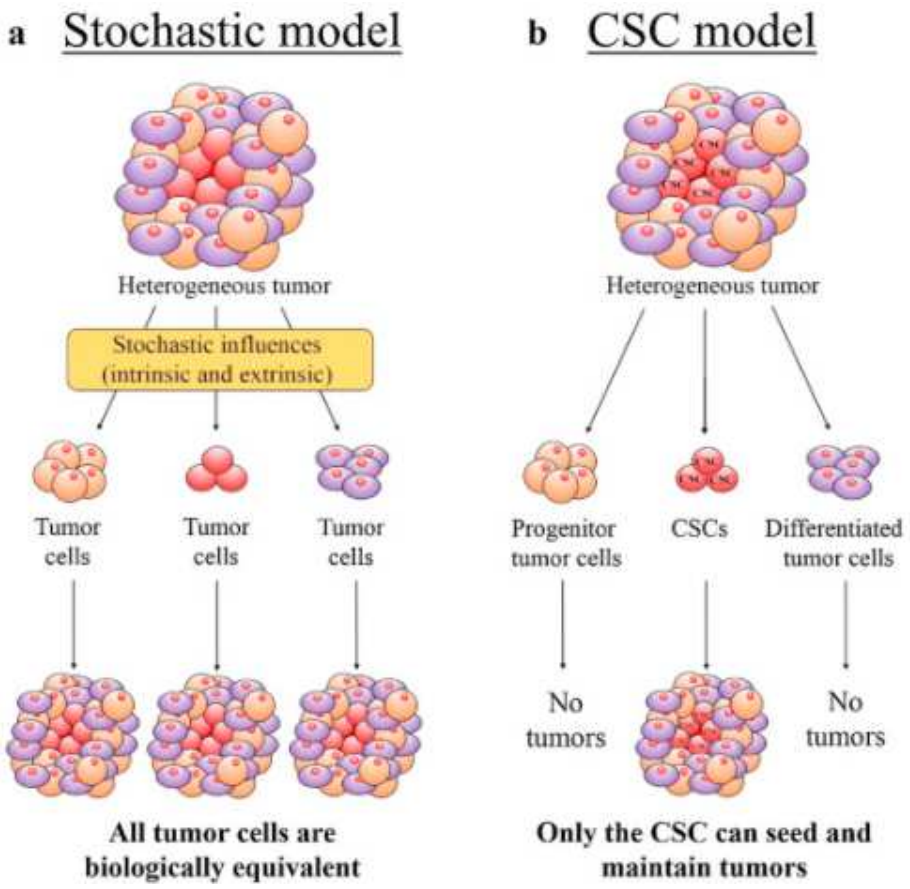

Figure 1. Models of cellular heterogeneity in solid tumors. Tumors are composed of a heterogeneous population of cells with different phenotypic characteristics. Different cell types are shown in different colors; (A) stochastic model: all tumor cells are biologically equivalent and have equal tumorigenic capacities. The behavioral variation is the result of intrinsic and extrinsic stochastic influences; (B) Cancer stem cell hypothesis: only a subpopulation of tumor cells (CSC, in red) is able to self-renew and originate new tumors (KOREN; FUCHS, 2016).

In normal tissues, stem cells (SC) are defined as immature and non-specialized cells that display a unique ability to self-renew and differentiate into specialized cells in an attempt to maintain tissue integrity (EGUSA; SONOYAMA; NISHIMURA; ATSUTA *et al.*, 2012; LEMISCHKA, 2005; VALENT; BONNET; DE MARIA; LAPIDOT *et al.*, 2012). CSC have similar properties to SC and they were identified as an essential source of tumor cells in

different malignancies, such as in oral cancer (ERAMO; LOTTI; SETTE; PILOZZI *et al.*, 2008; O'BRIEN; POLLETT; GALLINGER; DICK, 2007; RODINI; LOPES; LARA; MACKENZIE, 2017). Importantly, these cells are chemoresistant and capable to propagate and support tumorigenesis (DAWOOD; AUSTIN; CRISTOFANILLI, 2014; SHIGDAR; LI; BHATTACHARYA; O'CONNOR *et al.*, 2014). According to Singh *et al*. (2003), the ability to initiate tumors and originate heterogeneous cell populations found in the original tumor are exclusive properties of CSC. In view of that, it is important to develop specific therapies targeting CSC for cancer treatment.

The first evidence of CSC in tumor progression was demonstrated when human leukemic tumor cells were xenografted in non-obese diabetic/severe combined immunodeficient (NOD/SCID) mice, and only $CD34^{+}/CD38^{-}$ cells were capable to initiate tumor growth (BONNET; DICK, 1997). Thereafter, CSC were identified by specific markers in solid brain tumors ($CD133^{+}$ cells) (SINGH; CLARKE; TERASAKI; BONN *et al.*, 2003), breast tumors ($CD44^{high}/CD24^{low}/ESA^{+}$) (AL-HAJJ; WICHA; BENITO-HERNANDEZ; MORRISON *et al.*, 2003), prostate tumors ($CD44^{+}$) (PATRAWALA; CALHOUN; SCHNEIDER-BROUSSARD; LI *et al.*, 2006) and oral tumors ($CD44^{+/high}$) (LOCKE; HEYWOOD; FAWELL; MACKENZIE, 2005; PRINCE; SIVANANDAN; KACZOROWSKI; WOLF *et al.*, 2007). Researchers also identified CSC by the high activity of the aldehyde dehydrogenase enzyme (ALDH1) in breast and oral cancers (CLAY; TABOR; OWEN; CAREY *et al.*, 2010; GINESTIER; HUR; CHARAFE-JAUFFRET; MONVILLE *et al.*, 2007).

The subsequent studies on CSC biomarkers revealed that this subpopulation is significantly involved with tumor behavior. BMI1 (also known as B-lymphoma Moloney murine leukemia virus insertion region 1) is involved in the self-renewal, differentiation and initiation of brain and prostate tumors (ABDOUH; FACCHINO; CHATOO; BALASINGAM *et al.*, 2009; LUKACS; GOLDSTEIN; LAWSON; CHENG *et al.*, 2010). Overexpression of BMI1 in an $ALDH1^{+}$ subpopulation was correlated with increased tumor formation, cell migration, local invasion, and metastasis in head and neck squamous cell carcinoma (HNSCC) (YU; LO; CHEN; HUANG *et al.*, 2011). This suggests that presence of BMI1 can be used as a predictive marker of CSC in addition to CD44 and ALDH1.

Research of our group is investigating the role of CSC and tumor microenvironment in OSCC development and progression (Young Investigator Grant, FAPESP # 2013/07245-9). Recently, we found that CD44 immunoexpression was associated with lymph node metastasis,

while high expression of ALDH1 was associated with angiolymphatic invasion (ORTIZ; LOPES; AMÔR; PONCE *et al.*, 2018).

1.3 Epithelial-mesenchymal transition

The epithelial to mesenchymal transition (EMT) is a biological process involved in early stages of embryonic development. Epithelial cells loss apical-basal polarity and intercellular junctions, acquiring a mesenchymal phenotype that enables them to migrate beyond the primary site to integrate into surrounding or distant tissues (PARSANA; AMEND; HERNANDEZ; PIENTA *et al.*, 2017). Importantly, studies have demonstrated that carcinoma cells undergo EMT, acquiring migratory and- invasive properties, which are a critical step during tumor metastasis events (FEDELE; CERCHIA; CHIAPPETTA, 2017; THIERAUF; VEIT; HESS, 2017).

Notably, CSC undergo EMT mediated by cell transcription factors (SLUG, SNAIL and TWIST) activated in response to WNT signaling pathways, leading to intracellular changes such as hyperregulation of vimentin expression, inhibition of E-cadherin expression and nuclear translocation of β-catenin (THIERY, 2003). In OSCC, Biddle *et al*. identified two distinct phenotypes of CSC: one described as proliferative with epithelial characteristics, $CD44^{High}ESA^{High}$; and another with migratory traits, $CD44^{High}ESA^{Low}$, which exhibits mesenchymal properties. Consequently, it is worth to emphasize the role of biomarkers to identify these phenotypes as a target in further cancer therapies (BIDDLE; LIANG; GAMMON; FAZIL *et al.*, 2011).

Liu *et al*. investigated the immunoexpression of EMT-related proteins in tongue squamous cell carcinoma (TSSC). SNAIL, E-cadherin, N-cadherin, and Vimentin were associated with tumorigenesis and pathological outcomes. Vimentin was described as a potential prognostic factor for TSCC patients (LIU; KANG; WU; SUN *et al.*, 2017). In a different study, SNAIL expression in HNSCC was correlated with metastasis and poor prognosis (YANG; CHANG; CHIOU; LIU *et al.*, 2007). Reduced E-cadherin expression at the invasive tumor front suggest that this transmembrane glycoprotein is a noteworthy EMT marker in OSCC (COSTA; LEITE; CARDOSO; LOYOLA *et al.*, 2015). Moreover, high expression of N-cadherin has been correlated to enhanced tumor cell invasion and migration, leading to tumor

growth in carcinomas (SMITH; TEKNOS; PAN, 2013). Thus, SNAIL, E-cadherin, N-cadherin, and Vimentin expression is well recognized and established as EMT markers.

1.4 Experimental models of tumorigenesis *in vivo*

The most used protocol for experimental models of tumorigenesis *in vivo* involves the use of chemical agents as carcinogens. DMBA (9, 10-dimethyl-1, 2-benzanthracene) and 4NQO (4-nitroquinoline 1-oxide) are the most used in oral experimental chemical carcinogenesis. DMBA causes DNA adduct formation, failure in the repair of which leads to the development of cancer (MAAYAH; GHEBEH; ALHAIDER; EL-KADI *et al.*, 2015). DMBA also promotes local irritation, resulting in inflammatory response and necrosis. Thus, early epithelial lesions become difficult to analyze (KANOJIA; VAIDYA, 2006; RAJU; IBRAHIM, 2011). On the other hand, 4NQO is a water-soluble agent, which induces tumors in the oral cavity with histological and molecular changes similar to oral carcinogenesis in humans (VERED; YAROM; DAYAN, 2005). This model often results in multiple lesions, which enables to study all stages of tumorigenesis, including dysplasia, invasive tumor at the primary site and metastasis. However, this model includes a long time for tumor development (at least 48 weeks), the size and the number of tumors are hardly reproducible among replicates, and the mice display low rate of lymphatic metastasis (SZANISZLO; FENNEWALD; QIU; KANTARA *et al.*, 2014).

The gold-standard method applied in the study of CSC phenotype is the xenoimplatation of human tumor cells into immunocompromised animals (SCHATTON; FRANK, 2010). This experimental model generates lesions that displays similarities to the cellular and molecular changes which occur during the development and progression of OSCC in humans (RAJU; IBRAHIM, 2011). In addition, animal models can be used for the development of biological markers for diagnosis and prognosis of the disease (KANOJIA; VAIDYA, 2006).

Immunoexpression of CD44, ALDH1 and BMI1 have been reported as potential prognostic markers in OSCC. In view of the mutual relationship between CSC and EMT in tumor progression, EMT-related proteins (E-cadherin, SNAIL and Vimentin) might be relevant biomarkers in the study of CSC phenotypes. Therefore, we aimed to induce tumorigenesis by xenoimplantation of the CSC subpopulations ($CD44^{High}ESA^{High}$ and $CD44^{High}ESA^{Low}$ into the

tongue of NOD/SCID mice. Further, formed tumors were characterized microscopically by H&E and submitted to immunohistochemistry for the above-mentioned markers.

2 ARTICLE

2 ARTICLE

Pathology – Research and Practice

Microscopic and immunohistochemical characterization of tumor development in immunocompromised mice xenografted with cancer stem cells of oral squamous cell carcinoma

Rodrigo Fonseca Buzo[1], Nádia Ghinelli Amôr[1], Rafael Carneiro Ortiz[1], Nathália Martins Lopes[1], Luciana Mieli Saito[1], Camila de Oliveira Rodini[1].

1. School of Dentistry of Bauru, University of Sao Paulo (FOB/USP) – Department of Biological Science, Bauru, Brazil;

***Corresponding author**
Camila de Oliveira Rodini Pegoraro
Bauru School of Dentistry (FOB/USP) - Department of Biological Sciences
Al. Octávio Pinheiro Brisola, 9-75 - CEP 17012-901 – Bauru - SP - Brazil
Phone +55 (14) 3226-6126
Email: carodini@usp.br

CONFLICT OF INTEREST DISCLOSURE: The authors declare no conflict of interest.

LIST OF ABREVIATIONS

OSCC	Oral Squamous Cell Carcinoma
ITF	Invasive Tumor Front
CSC	Cancer Stem Cells
NOD/SCID	Non-obese Diabetic/severe Combined immunodeficient
ALDH1	Aldehyde Dehydrogenase Enzyme 1
BMI1	B-lymphoma Moloney murine leukemia virus insertion
HNSCC	Head and Neck Squamous Cell Carcinoma
CD44	Principal cell surface receptor for hyaluronate
IHC	Immunohistochemistry
DMEM	Dulbecco's modified Eagle's medium
FBS	Fetal Bovine Serum
RT	Room Temperature
H&E	*Hematoxylin and eosin* stain

ABSTRACT

Oral squamous cell carcinoma (OSCC) is one of the most common neoplasms of the head and neck region, with overall survival <5 years. The worst prognosis of the disease is lymph node metastasis associated with a subpopulation of stem cells in tumors, known as cancer stem cells (CSC). Studies have shown that this subpopulation undergoes epithelial to mesenchymal transition (EMT), a process which epithelial cells acquire a mesenchymal phenotype. In OSCC, CSC can be identified by biomarkers, CD44 transmembrane protein being the most *commonly* used. In oral cancer research, animal models have been widely used as a strategy to understand carcinogenesis as well as to test new antineoplastic agents and to develop new therapeutic approaches. We aimed to evaluate and compare microscopically murine tumors induced by CSC xenotransplantation. Two subpopulations $CD44^{High}ESA^{High}$ (epithelial) and $CD44^{High}ESA^{Low}$ (mensenchymal) were isolated from OSCC cell line LUC4 by flow cytometry (BD FACSAria ™ Fusion). Xenotransplantation was performed with $5x10^3$ cells injected in the tongue into two groups with twelve NOD/SCID mice each one. Forty-nine days post-injection, tumors were measured, collected and submitted to histotechnical processing for microscopic and immunohistochemical analyses. $CD44^{High}ESA^{High}$ cells showed great tumorigenic potential, being able to originate larger tumors in twelve animals (average tumor area: 4.22 mm²). In contrast, only six animals (50%) xenografted with $CD44^{high}ESA^{low}$ cells developed microscopically visible tumors (average tumor area: 0.20 mm²). Structural and cellular changes similar to the human OSCC were observed in both groups. In addition, animals xenografted with $CD44^{High}ESA^{High}$ cells showed greater weight loss compared to the $CD44^{High}ESA^{Low}$ group ($p = 0.0217$). The correlation of CSC subpopulations with their corresponding tumors *in vivo* represents a reliable approach for future research in oral cancer, highlighting the role of different CSC phenotypes in OSCC development and progression. Further studies should be conduct in this field, for example, in understanding how they respond in commonly used therapeutics and develop techniques to overcome their resistance mechanisms.

Keywords: Oral Squamous Cell Carcinoma. Cancer Stem Cells. Epithelial-Mesenchymal Transition. Immunocompromised Mice.

1. Introduction

Oral squamous cell carcinoma (OSCC) is the most frequent cancer of oral cavity, representing almost 90% of all cases. It is well recognized as a worldwide health problem due to high ability to metastasize into cervical lymph nodes, reaching high mortality and morbidity rates [1-3]. OSCC etiological factors include mostly tobacco and alcohol habits, associated with patient genetic predisposition [4]. Despite the advances in treatment and diagnosis, it is not well characterized which molecular pathways are exactly involved in OSCC tumorigenesis [5].

Current evidence suggests that a small population of cancer cells known as cancer stem cells (CSC) drives tumor growth, being involved in metastasis, cancer recurrence and resistance to chemotherapy [6]. Additionally, CSC are linked to poor prognosis and aggressive behavior in OSCC [7, 8]. Therefore, targeting CSC might be an essential therapeutic approach for cancer treatment.

Studies have demonstrated that CSC can be identified by the expression of some biomarkers in OSCC, such as CD44, ALDH1 and BMI1 [9-11]. Ortiz *et al*. (2018) found an association of CD44 and ALDH1 immunoexpression in OSCC and cervical lymph node metastasis and angiolymphatic invasion, respectively [12]. In a different study, BMI1 expression in $ALDH1^{+}$ subpopulation of head and neck squamous cell carcinoma (HNSCC) was correlated with tumor growth, cell migration and local invasion [13]. Once the expression of CD44, ALDH1 and BMI1 is related to OSCC poor prognosis, these CSC molecular biomarkers might become targets for developing new therapies in oral cancer.

It has been pointed out that CSC undergo epithelial to mesenchymal transition (EMT) mediated by cell transcription factors (SLUG, SNAIL and TWIST) in response to WNT signaling pathways [14]. EMT then enables CSC to migrate and invade adjacent tissues by downregulation of epithelial proteins, such as E-cadherin, and upregulation of mesenchymal proteins, such as Vimentin [15, 16]. Recently, Zhou *et al*. (2015) reported that decreased expression of E-cadherin and increased expression of Vimentin were positively associated with lymph node metastasis [17]. Notably, CSC undergoes EMT while retaining their stem-like properties. In fact, Biddle *et al*. (2011) identified two distinct CSC phenotypes: one described as proliferative with epithelial characteristics, classified as $CD44^{High}ESA^{High}$ (Epi-CSC); and another one with migratory traits, classified as $CD44^{High}ESA^{Low}$ (EMT-CSC), which exhibits mesenchymal properties [18].

In oral cancer research, animal models have been widely used as a strategy to understand carcinogenesis as well as to test novel antineoplastic agents and develop new therapeutic approaches [19]. According to Clarke *et al*. (2006), xenotransplantation of CSC into non-obese diabetic/severe combined immunodeficient (NOD/SCID) mice in an orthotopic site is the gold-standard assay in CSC study [20]. In fact, orthotopic xenograft is a relevant model due to similarities with cellular and molecular changes in human carcinomas development and progression, mimicking tumor microenvironment conditions [21, 22]. Based on these observations, we aimed to analyze the *in vivo* behavior of different CSC phenotypes from LUC4 OSCC cell line injected in the tongue of 24 NOD/SCID mice. Also, a detailed microscopic analysis of tumor development and immunohistochemistry (IHC) of CSC (CD44, ALDH1 and BMI1) and EMT-related markers (E-cadherin, Vimentin and SNAIL) was performed. To our knowledge, this is the first work focused on the characterization of the *in vivo* model of OSCC induced by different CSC phenotypes.

2. Material and methods

2.1. Cell line

Primary OSCC-derived cell line LUC4 [18] was cultured in RM+ medium which is composed by 3:1 mixture of Dulbecco's modified Eagle's medium (DMEM) and Ham's F12 medium supplemented with 10% fetal bovine serum (FBS), 1% antibiotics and antimycotics and mitogens [23]. Cells were maintained at 37ºC in a humidified atmosphere 5% CO_2 / 95% air. The culture medium was changed every 24-72h and the subculturing was practiced whenever necessary.

2.2. Flow cytometry and fluorescence-activated cell sorting (FACS)

$CD44^{High}ESA^{High}$ (Epi-CSC) and $CD44^{High}ESA^{Low}$ (EMT-CSC) subpopulations were FACS-sorted for *in vivo* tumorigenesis assays. Briefly, LUC4 whole population was detached, washed and incubated with fixable viability stain (1:3 000, BD Horizon™) for 15 minutes at room temperature (RT). Then, tumor cells were simultaneously incubated with mouse anti-human PerCP-Cy™5.5-CD44 (2:100, clone G44-26, BD Pharmingen™) and mouse anti-human BV605-CD326 (2:100, clone EBA-1, BD Pharmingen™) antibodies for 30 minutes at 4ºC in the dark. Samples were washed with phosphate buffered saline pH 7.2 (Gibco™) and

FACS-sorted using BD FACSAria^{TM} Fusion Cell Sorter (BD Biosciences) based on CD44 and ESA expression levels. CSC subpopulations were collected into RM^{+} medium supplemented with 20 % FBS and 10 % antibiotic/antimycotic at RT.

2.3. Animals

The study was conducted in 24 NOD/SCID mice (6-8 week-old, male) obtained from the Animal Facility at University of São Paulo Medical School. Animal care was complied with Ethics Committee on Animal Use (School of Dentistry, University of São Paulo, #002/2017).

2.4. Xenograft model

Immediately after sorting, tumor cells were washed and post-sorting viability was analyzed by trypan blue exclusion. Cell concentration was adjusted to $5x10^3$ cells in 30µL of Matrigel® Matrix (Corning®). Then, tumor cells were transplanted into the tongue of anesthetized NOD/SCID mice. Animals were divided in two groups according to CSC subpopulation: LUC4 $CD44^{High}ESA^{High}$ (group 1, n = 12) and LUC4 $CD44^{High}ESA^{Low}$ (group 2, n = 12). Tumor development and animals' survival were monitored throughout the protocol execution. Chow intake and mice weight were also monitored weekly for possible changes in habit.

2.5. Euthanasia and tumor tissue samples

Animals were euthanized by overdose of anesthetics intraperitoneally 49 days post-injection, considering animals' compromised health by low weight. Mice tumors were collected and fixed in 10% *formaldehyde.* Samples were submitted to histotechnical processing and paraffin inclusion for further H&E and IHC analysis.

2.6. Macroscopic and microscopic analyses

Xenograft tumors were described based on clinical features of lesions, according to aspects of anatomic site, number (single or multiple), size, shape, border, surface, base and color of lesions.

Histopathological analyses of the tumors were carried out in accordance with World of Health Organization [24]. Specifically, cellular and architectural alterations were evaluated. The number of typical and atypical mitosis and the invasion grade, including the invasion by clusters or tumor as whole, was used to characterized xenograft tumors. We evaluated degrees of squamous differentiation: well-differentiated areas characterized by abundant keratin pearls formation; moderately differentiated areas with less keratinization, exhibiting distinct nuclear pleomorphism and mitotic activity; and poorly- or undifferentiated areas characterized by predomination of immature cells and minimal keratinization.

For IHC, sections were dewaxed with xylene and rehydrated in graded ethanol solutions. Heat-induced epitope retrieval was performed in a pressure cooker (Decloaking Chamber^{TM} NxGen, Biocare Medical) using citrate-buffer solution pH 6.0 (SigmaAldrich) at 110°C for 5 minutes. Then, sections were incubated in 3% hydrogen peroxide for 10 minutes to block endogenous peroxidase activity followed by Protein Block Serum-Free (Dako, Carpinteria, CA) for 15 minutes at RT to suppress nonspecific binding of subsequent reagents. Tissue sections were incubated with primary antibodies and, after washing, incubated with specific detection reagents (Table 1). Finally, sections were stained with 3,3'-Diaminobenzidine and counterstained with Mayer's hematoxylin.

Slides were further scanned into high-resolution images using the Aperio Scanscope CS Slide Scanner (Aperio Technologies Inc, Vista, CA, USA). All digital images obtained in .svs format were visualized with ImageScope software (Aperio Technologies Inc). The algorithm PixelCount V9 (Aperio Technologies Inc) was used to analyse the expression of CSC and EMT markers.

2.7. Statistics

Statistical analyses were performed using GraphPad Prism 5 (GraphPad Software, Inc., CA, USA). We compared CSC and EMT markers expression between the two groups by Unpaired *t*-test. Correlations between all markers were assessed by Pearson's correlation coefficient test in $CD44^{High}ESA^{High}$ tumors. P values <0.05 were considered statistically significants.

3. Results

3.1. *Epi-CSC have higher tumorigenic potential in vivo than EMT-CSC*

In cell culture, LUC4 lineage showed two different morphologies: one exhibiting spherical nuclear morphology mostly arranged in groups, typically epithelial morphology) and another one showing elongated cytoplasm with fibroblast-like appearance as individual cells often observed in cells in EMT (Fig. 1A). To better characterize the phenotype of these cells, we analyzed CD44 (CSC marker) and ESA (epithelial-specific antigen) staining by flow cytometry (Fig. 1B, C). We identified two subpopulations of LUC4 cells: $CD44^{High}ESA^{High}$ (named Epi-CSC) and $CD44^{High}ESA^{Low}$ (EMT-CSC) (Fig. 1B-C). Our results demonstrated that LUC4 OSCC cell line is preferentially composed by EMT-CSC (Fig. 1C).

To compare the tumorigenic abilities of both subpopulations, immediately after sorting, Epi- and EMT-CSC were inoculated into the tongues of immunocompromised mice (NOD/SCID mice). Forty-nine days post-injection, macroscopic tumors observed were well-circumscribed single nodular lesions deeply located in muscle tissue of tongue's anterior region, exhibiting sessile base, defined contour and slighty whitish-colored surface (Fig. 2A-C). In addition, we found three cases with bilateral growth and two cases with ulcerated surface. As expected, 100% of Epi-CSC xenografted-mice developed macroscopic tumors (Fig. 2D). On the other hand, only 41.6% of mice inoculated with EMT-CSC cells displayed macroscopic tumors (Fig. 2D). In addition, tumors formed from Epi-CSC cells were larger (average tumor area: 4.22 mm^2) and exhibited higher volume than EMT-CSC-derived tumors (average tumor area: 0.20 mm^2) (Fig. 2E). In fact, animals inoculated with Epi-CSC had greater weight loss compared to EMT-CSC-xenografted animals (Figure 2F), reflecting the increased tumor development observed in Epi-CSC-xenografted mice.

3.2. Histopathological analyses of xenografted-derived tumors

Despite the bigger tumor volume observed in Epi-CSC inoculated mice, both CSC subpopulations were able to generate squamous cell carcinomas in the tongue with similar cellular and structural alterations found in human OSCC.

Epi-CSC originated large tumors as exophytic masses, promoting ulcerated areas as expected (Fig. 3A). Central areas of Epi-CSC carcinomas exhibited well-differentiated grade with keratin pearl and tumor islets formation (Fig. 3B). Moderately- (Fig. 3C) and poorly- (Fig.

3D) differentiated areas were also observed in Epi-CSC-derived tumors. Compatible to human carcinomas, we found a considerable number of altered nuclear-cytoplasmic ratio (data not shown) and mitotic activity, including abnormal mitoses (Fig. 3C) in Epi-CSC-derived tumors. Regarding the invasive tumor front (ITF), tumor cell clusters were found in deep muscle tissue (Fig. 3E and F).

On the other hand, EMT-CSC generated smaller tumors classified as well-differentiated with keratin pearl formation (Fig. 3G). Dysplasia was also observed in EMT-CSC-derived tumors such as hyperchromatic nuclei (Fig. 3H) and presence of multinucleate cells (Fig. 3I). At the ITF, malignant cells apparently migrating toward perineural regions were observed (Fig. 3J).

3.3. *CSC markers in xenografted-derived tumors*

To evaluate whether immunolabeling pattern of human OSCC reflects upon xenografted-derived tumors in mice, we evaluated by IHC the immunostaining of well-established human CSC markers: CD44, ALDH1, and BMI1 (Fig. 4). Concerning cellular location of each marker, as expected, tumor generated by both subpopulations displayed membrane staining of CD44, meanwhile ALDH1 were cytoplasmatic and BMI1 were detected at nucleus level (Fig. 4).

CD44 showed great reactivity throughout tumor extension of Epi-CSC-derived carcinomas; however, we observed downregulation of this protein at the center of some tumor islets (Fig. 4A). Notably, CD44 exhibited remarkable expression at the ITF (Fig. 4B). Similarly, CD44 immunolabeling of tumors generated by EMT-CSC inoculation was upregulated on tumor islets periphery (Fig. 4C). There was no significant difference in the immune staining intensity of CD44 when comparing tumors generated by Epi-CSC and EMT-CSC (Fig. 4D).

ALDH1 showed focal staining unrestricted to tumor cells cytoplasm due to nuclear translocation on both tumor groups (Figure 4E-G). In addition, ALDH1 immunopositivity was reduced in tumors periphery and ITF (data not shown). Again, both tumor groups displayed similar immunolabeling intensity of ALDH1 (Fig. 4H).

BMI1 expression was uniform with great nuclear labeling widely distributed in tumors generated from Epi-CSC in central areas (Fig. 4I) and in clusters of tumor cells at the ITF (Fig. 4J), as well in EMT-derived tumors (Fig. 4K). However, BMI1 staining was significantly more intense in Epi-CSC derived tumors compared to tumors generated from EMT-CSC cells (Fig. 4L).

3.4. *EMT markers in xenografted-derived tumors*

We evaluated the presence of EMT biomarkers on tumors generated from the xenografted mice. Similar to human OSCC, in tumors generated from both CSC subpopulations, E-cadherin, Vimentin, and SNAIL immunostaining were observed in membrane, cytoplasm and nuclei of tumor cells, respectively (Fig. 5).

As expected in Epi-CSC carcinomas, E-cadherin immunopositivity was intense in central area (Fig. 5A). However, at the ITF, immunostaining was not that evident (Fig. 5B). Interestingly, intense membrane staining of E-cadherin was also detected in EMT-CSC-derived tumors (5C). Indeed, no significant difference was detected comparing immunostaining intensity of E-cadherin from tumors generated from Epi- and EMT-CSC (Fig. 5D).

Vimentin expression in carcinomas derived from Epi-CSC cells was higher at the periphery and decrease of labeling was detected in central areas (Fig. 5E). Conversely, Vimentin was highly stained at the ITF in tumors generated from Epi-CSC subpopulation (Fig. 5F). Controversially, Vimentin staining was lower in EMT-CSC-derived tumors (Fig. 5G-H).

Finally, SNAIL was highly expressed at central areas in tumor cells nuclei from both tumors, Epi- and EMT-CSC-derived (Fig. 5I-J), with no significant difference between both tumors (Fig. 5K).

3.5. *Correlation analysis of CSC and EMT biomarkers*

Correlation analysis is frequently used to measure the strength of the relationship between two variables. In Epi-CSC carcinomas, we found positive correlations between BMI1 and ALDH1 (Fig. 6A), CD44 and Vimentin (Fig. 6B), and E-cadherin and Vimentin (Fig. 6C) markers. There was no significant correlation between immunohistochemical markers in tumors derived from EMT-CSC (data not shown).

4. Discussion

Recent studies have demonstrated a large number of promising markers in OSCC prognosis [25, 26]. Targeting CSC have been used as a pathway to identify OSCC high-risk cases to overcome cancer progression and improve the therapeutic outcomes [27]. Although the well-recognized limitations, animal models represent a fundamental tool for cancer research once they allow the understanding and manipulation of every step of tumorigenesis, such as

initiation, promotion, progression, and metastasis, as well the discover of new drugs [19, 22]. Based on that, the development of a reliable *in vivo* model that resembles human OSCC behavior improves the translational research success. Taking advantage of xenograft mice model, the present study evaluated OSCC development and assessed the well-stablished CSC (CD44, ALDH1, and BMI1) and EMT (E-cadherin, Vimentin, and SNAIL) makers by IHC in OSCC-derived tumors in NOD/SCID mice to determine whether human carcinomas dysplastic characteristics and immunolabeling pattern reflects upon xenografted tumors.

When xenografted into the tongues of NOD/SCID mice, both LUC4 Epi-CSC and EMT-CSC subpopulations were able to generate microscopic tumors *in vivo* corroborating the notion that $CD44^{+}$ cells possess tumorigenic potential, therefore are CSC. In fact, in an orthotopic mouse model of oral cancer, SCC9 $CD44^{High}$ cells were more tumorigenic and capable to originate heterogeneous tumors when compared with $CD44^{Low}$ cells [28]. However, we observed that Epi-CSC showed higher capacity to colonize the primary site of inoculation and they formed larger tumors *in vivo* than EMT-CSC cells. Al-Hajj et al. (2003) obtained similar results by xenotransplanting human breast cancer cells $ESA^{+}CD44^{+}CD24^{-}$ in immunocompromised mice [29]. More importantly, Sen and Carnelio (2016) demonstrate that ESA-positive OSCC are correlated with worst prognosis being associated with tumor size, histological grade and survival [30]. Then, our *in vivo* model reflects clinical findings demonstrating that $CD44^{High}$ cells exhibiting high levels of the epithelial marker, ESA, are tumorigenic and consequently, might be a potential biomarker for OSCC.

Besides tumorigenic capacity, we also need to determine whether xenografted tumors displayed histopathological similarities with human OSCC. OSCC is formed by neoplastic epithelial cells that display distinct stages of squamous differentiation [31]. Malignant cells exhibiting disordered growth, keratin pearls formation, altered nuclear-cytoplasmic ratio, nuclear chromatin irregularities and increased mitotic figures are the most common findings in OSCC [32]. Forty-nine days post-injection, tumors derived from both CSC subpopulations presented OSCC traits, such as: *islet*s of tumor cells with keratin pearl formation, distinct nuclear pleomorphism, hyperchromasia, abnormal mitoses and multinucleated cells. These results suggest that xenograft-derived tumors, mostly Epi-CSC-derived tumors, resemble closely to architectural and cellular changes found in human OSCC.

Regarding CSC markers, tumors generated by both CSC subpopulations preserved the immunoexpression of CD44 and displayed similar cytoplasmatic expression of ALDH-1, demonstrating that tumor cells conserved their CSC phenotype. Interestingly, we observed that BMI1 was higher stained in tumors derived from Epi-CSC than EMT-CSC. Hu *et al*. (2019)

showed that BMI1 is highly expressed in OSCC CSC and its inhibition attenuates oral CSC self-renewal and tumor-initiating potential [33]. Importantly, Bansal *et al*. (2016) demonstrated that inhibition of BMI1 in patient-derived cells decreased colony formation *in vitro* and tumor initiation *in vivo in prostate cancer [34]*. Notably, Feng *et al*. (2013) indicated that the co-expression of BMI1 and ALDH1 in oral erythroplakia was a strong indicator associated with malignant transformation [35]. In a different study, Yu *et al*. (2011) demonstrated that HNSCC-ALDH1$^+$ cells had high levels of BMI1. In addition, stemness properties were enhanced in HNSCC-ALDH1$^-$ cells when BMI1 was overexpressed by SNAIL upregulation [13]. Likewise, we found a positive correlation between BMI1 and ALDH1 in Epi-CSC-derived tumors, proposing that they might be valuable predictors for evaluating the risk of oral cancer.

Metastasis is the major prognostic factor associated with OSCC [36] and increased expression of EMT markers are frequently associated with worst prognosis [37]. Although the EMT-CSCs were described as cells in EMT [18], tumors derived from EMT-CSC stained for E-cadherin and SNAIL in a very similar intensity to Epi-CSC-derived tumors. Controversially, we also showed that Vimentin was more present in Epi-CSC-derived carcinomas. Vimentin has been reported as a component of mesenchymal cells, but it is also highly found in non-mesenchymal cells, like epithelial cells in EMT process [38], suggesting that Epi-CSC injected into the tongue of mice might be entering in the EMT program. We also identified upregulation of CD44 and Vimentin at the ITF and both markers were significantly correlated in Epi-CSC carcinomas. Accordingly, in a mucoepidermoid carcinoma, Irani and Jafari (2018) found cancer cells at the ITF that were positive for both Vimentin and CD44, stablishing an association between these markers and cancer invasion [39]. We also showed a positive correlation between Vimentin and E-cadherin in Epi-CSC carcinomas. Yamashita et al. (2015) demonstrated that the co-expression of Vimentin and E-cadherin is associated with the most aggressive phenotype and poor prognosis in breast cancer [40]. Interestingly, Zhou *et al*. (2015) found that Vimentin and E-cadherin positive expressions were linked to OSCC metastases [17]. However, we were unable to detect cervical lymph node metastasis in order to precisely establish the association between these markers and invasion. Long-term protocols should be conducted to evaluate the ability of both CSC subpopulations to metastasize.

In conclusion, using the surface markers CD44 and ESA we isolated two different phenotypes of CSC from OSCC. Epi-CSC displayed high tumorigenic potential to form heterogeneous tumors into NOD/SCID mice 49 days-post inoculation. Moreover, these tumors reproduced histopathological and immunolabeling pattern similar to human OSCC suggesting that xenografting Epi-CSC into immunocompromised mice represent a trustworthy approach

for future oral cancer research. Correlating CSC subpopulations with their corresponding tumors *in vivo* might highlight the role of different CSC phenotypes in OSCC development and progression. Further studies should be conduct in this field, for example, in understanding how they respond in commonly used therapeutics and develop techniques to overcome their resistance mechanisms.

Acknowledgments

The authors would like to thank Danielle Santi Ceolin and Patrícia De Sá Mortagua Germino for their technical assistance. This study was supported by scholarships and grants from Fundação de Amparo à Pesquisa do Estado de São Paulo – FAPESP (2013/07245-9).

Conflicts of interest

The authors declare that there is no conflict of interest regarding the publication of this paper.

Figures and figures legends

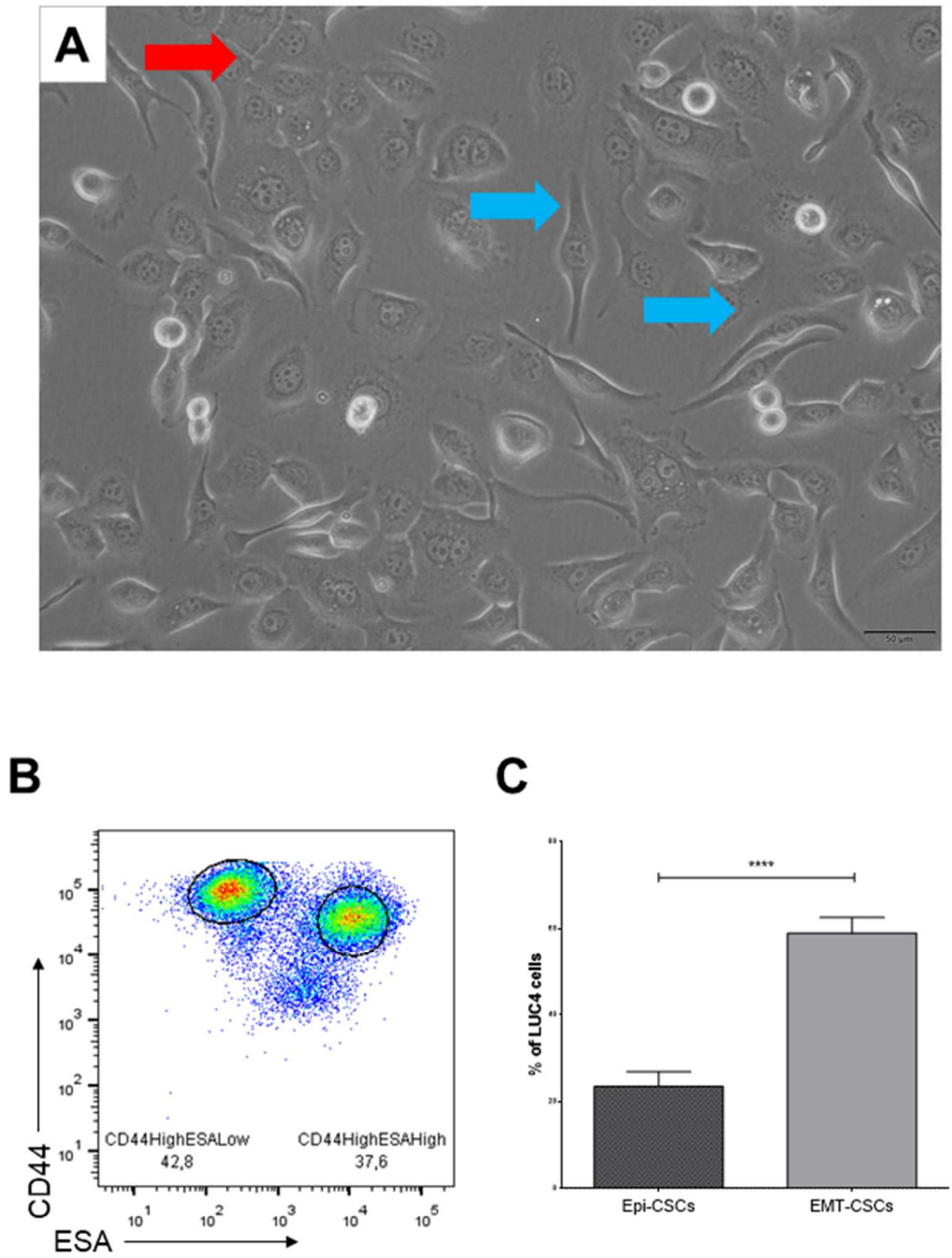

Fig. 1. LUC4 OSCC cell line is composed by two CSCs phenotypes. LUC4 cells were expanded until approximately 80% of confluence and CSCs phenotypes were FACS-sorted based on CD44 and ESA staining. (**A**) Photomicrograph of LUC4 cell culture showing the cellular morphology heterogeneity: group of cells with epithelial morphology (red arrow) and fibrobast-like morphology (blue arrows) (400x, scale bar: 50µm). (**B**) Dot plot showing the gate strategy for identification of epithelial ($CD44^{high}ESA^{high}$, Epi-CSCs) and mesenchymal subpopulation ($CD44^{high}ESA^{low}$, EMT-CSCs); and (**C**) respective quantification of each phenotype in LUC4 cell line. **** $p < 0.0001$.

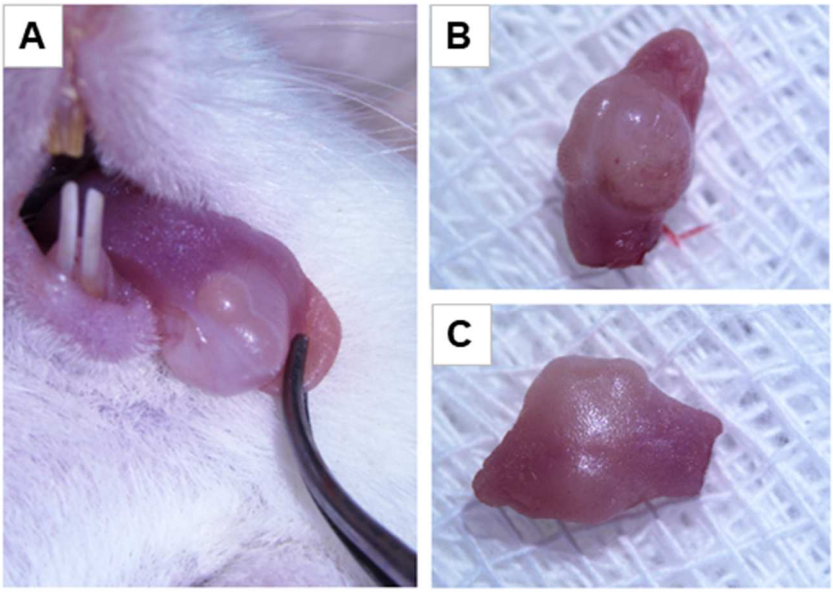

D

Subpopulation	Number of cells	Number of animals	Macroscopic tumor incidence	Microscopic tumor incidence
Epi-CSC	5 x 10^3	12	12 (100%)	12 (100%)
EMT-CSC	5 x 10^3	12	5 (41,6%)	6 (50%)

E **F**

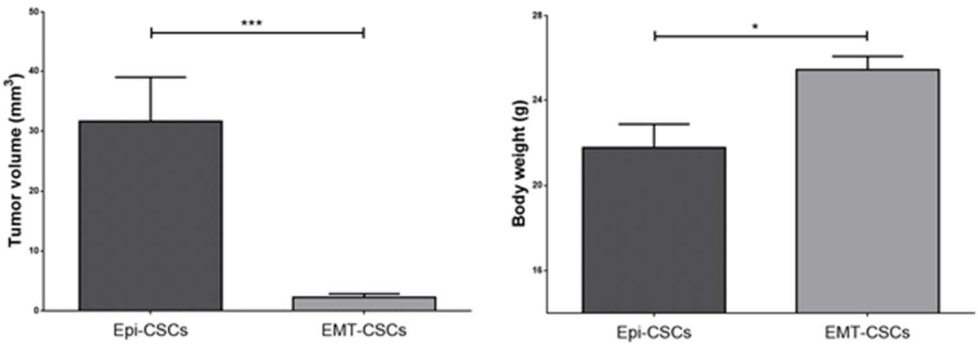

Fig. 2. LUC4 Epi-CSCs are highly tumorigenic *in vivo*. Immediately after sorting, both LUC4 CD44^{high} subpopulations were grafted into the tongue of 24 NOD/SCID mice. Tumor volume and mice's body weight were measured at the end of experimental protocol (49 days post-injection). (**A**-**C**) Macroscopic image of tumors derived from Epi-CSCs showing a nodular swelling at the anterior area of the tongue with well-defined contour and sessile base. (**D**) Macro and microscopic tumor invidence of LUC4 Epi-CSC and EMT-CSC inoculated subpopulations. Graphics showing (**E**) tumor volume and (**F**) body weight of xenografted mice at the end of the protocol. *** $p < 0.001$; *$p < 0.05$.

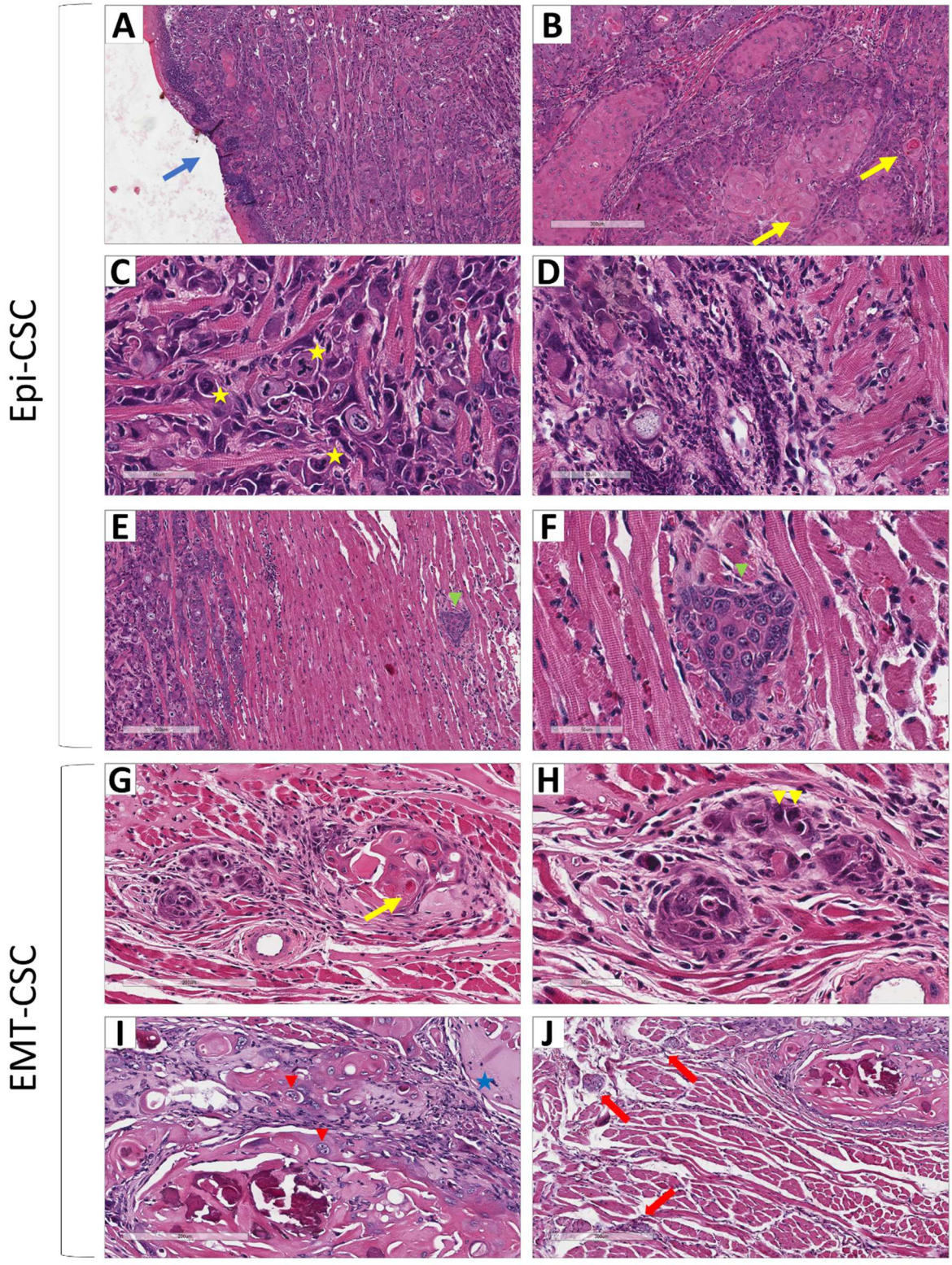

Fig. 3. Histopathological evaluation of OSCCs derived from Epi- and EMT-CSC cells. Forty-nine days post-injection, mice were euthanized and tumors were collected and processed for histopathological analyses. (**A-F**) H&E sections from Epi-CSC derived tumors demonstrating: ulcerated area (**A**, blue arrow; 40x); well-differentiated tumor with corneal pearls formation (yellow

arrow) and tumor islands (**B**, 100x, scale bar: 300μm); cell pleomorphism, nuclear hyperchromasia and atypical mitoses (yellow stars) in moderately (**está mais para pobremente**)-differentiated area (**C**, 400x, scale bar: 50μm); poorly-differentiated area (**D**, 400x, scale bar: 70μm); tumor cluster in deep muscle tissue (**E**, green arrowhead, 100x, scale bar: 200μm); and respective area with higher microscopic magnification (**F**, 400x, scale bar: 50μm). (**G-J**) H&E sections from EMT-CSC derived tumors demonstrating: well-differentiated area with corneal pearls (**G**, yellow arrow, 100x, scale bar: 200μm); cell pleomorphisim and nuclear hyperchromasia (**H**, yellow arrowhead, 400x, scale bar: 50μm); cellular multinucleation (red arrowhead) and remaining Matrigel (**I**, blue star, 100x, scale bar: 200μm), and perineural infiltration of small clusters of tumor cells (**J**, red arrows, 100x, scale bar: 300μm).

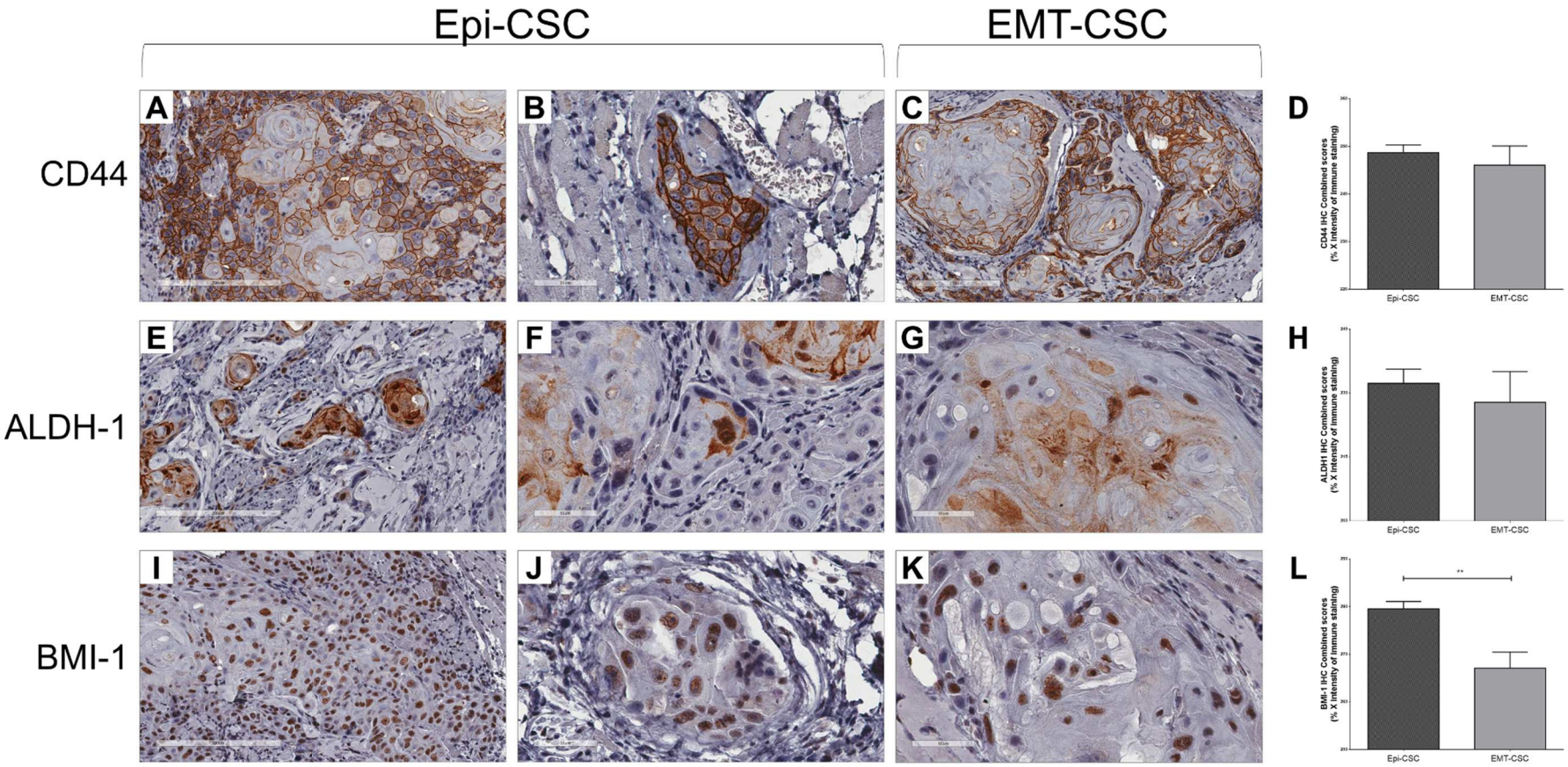
Epi-CSC
EMT-CSC
CD44
ALDH-1
BMI-1
A
B
C
D
E
F
G
H
I
J
K
L
CD44 IHC Combined scores
(% X Intensity of Immune staining)
ALDH1 IHC Combined scores
(% X Intensity of Immune staining)
BMI-1 IHC Combined scores
(% X Intensity of Immune staining)
Epi-CSC
EMT-CSC
**

Fig. 4. CSC biomarkers in xenografted-derived tumors. CD44 expression in (**A**-**B**) Epi-CSC-derived tumors (200x and 400x, scale bars: 200µm and 50µm, respectively), and in (**C**) EMT-CSC derived-tumors (100x, scale bar: 200µm). (**D**) Representative graphics comparing the immune staining intensity between Epi- and EMT-CSC derived tumors. ALDH-1 expression in (**E**-**F**) Epi-CSC-derived tumors (200x and 400x, scale bars: 200µm and 50µm, respectively) and in (**G**) EMT-CSC-derived tumors (400x, scale bar: 50µm). (**H**) Representative graphics comparing the immune staining intensity between Epi- and EMT-CSC derived tumors. BMI-1 expression in (**I**-**J**) Epi-CSC-derived tumors (200x and 400x, scale bars: 200µm and 50µm, respectively), and in (**K**) EMT-CSC derived-tumors (400x, scale bar: 50µm). (**L**) Representative graphics comparing the immune staining intensity between Epi- and EMT-CSC derived tumors. ** $p < 0.005$.

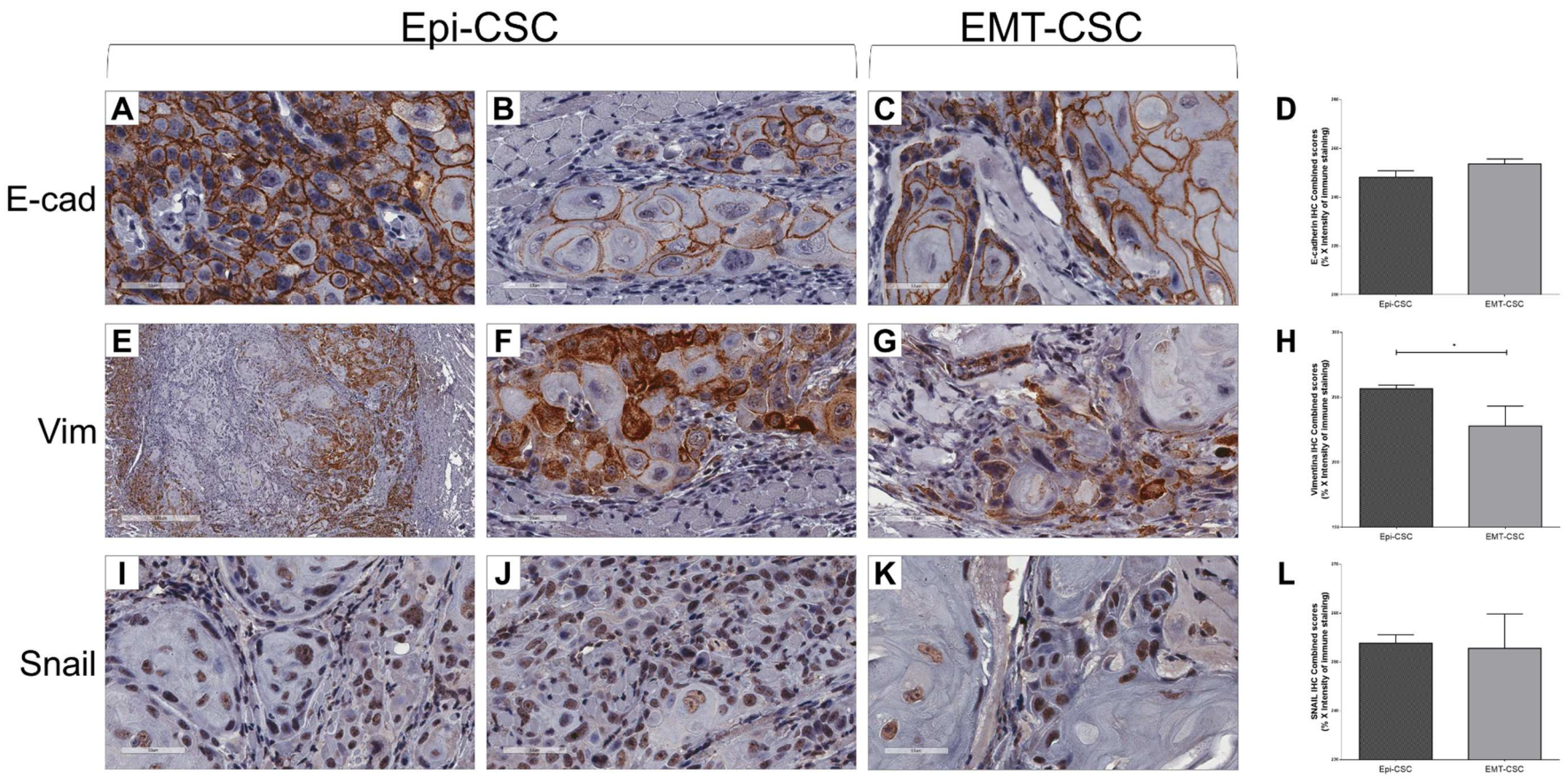
Epi-CSC
EMT-CSC
E-cad
Vim
Snail
A
B
C
D
E
F
G
H
I
J
K
L
E-cadherin IHC Combined scores
(% X Intensity of immune staining)
Vimentins IHC Combined scores
(% X Intensity of immune staining)
SNAIL IHC Combined scores
(% X Intensity of immune staining)
Epi-CSC
EMT-CSC
*

Fig. 5. EMT biomarkers in xenografted-derived tumors. E-cadherin expression in (**A**-**B**) Epi-CSC-derived tumors (400x, scale bar: 50µm), and in (**C**) EMT-CSC derived-tumors (400x, scale bar: 50µm). (**D**) Representative graphics comparing the immune staining intensity between Epi- and EMT-CSC derived tumors. Vimentin expression in (**E**-**F**) Epi-CSC-derived tumors (40x and 400x, scale bars: 500µm and 50µm, respectively) and in (**G**) EMT-CSC-derived tumors (400x, scale bar: 50µm). (**H**) Representative graphics comparing the immune staining intensity between Epi- and EMT-CSC derived tumors. Snail expression in (**I**-**J**) Epi-CSC-derived tumors (400x, scale bar: 50µm), and in (**K**) EMT-CSC derived-tumors (400x, scale bar: 50µm). (**L**) Representative graphics comparing the immune staining intensity between Epi- and EMT-CSC derived tumors. * $p < 0.05$.

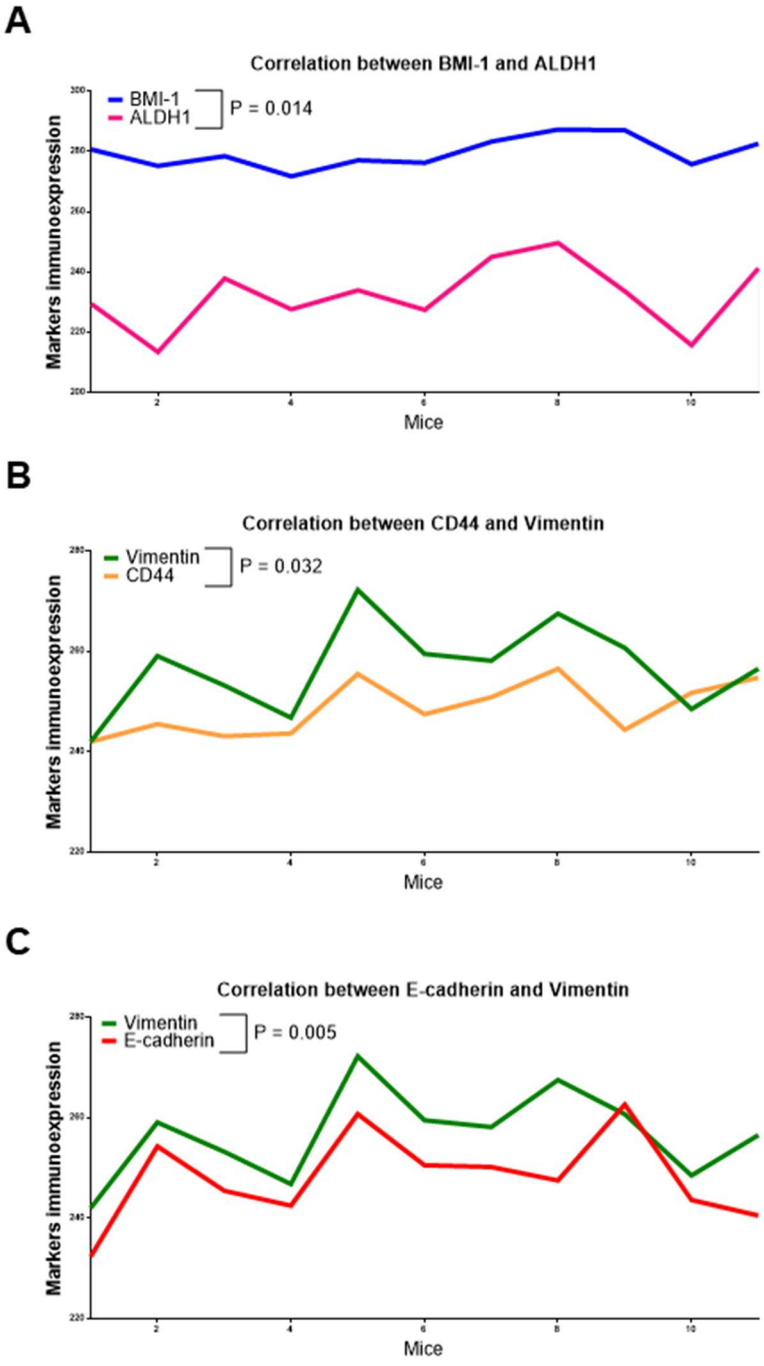

Fig. 6. Correlations of CSCs and EMT markers in Epi-CSCs xenografted-derived carcinomas. Correlation analyzes of (**A**) BMI-1 and ALDH1, (**B**) CD44 and Vimentin and (**C**) E-cadherin and Vimentin correlation.

References

[1] Beenken SW, Krontiras H, Maddox WA, et al. T1 and T2 squamous cell carcinoma of the oral tongue: prognostic factors and the role of elective lymph node dissection. *Head Neck*. 1999; 21: 124-30.

[2] Zini A, Czerninski R, Sgan-Cohen HD. Oral cancer over four decades: epidemiology, trends, histology, and survival by anatomical sites. *J Oral Pathol Med*. 2010; 39: 299-305.

[3] Lambert R, Sauvaget C, de Camargo Cancela M, et al. Epidemiology of cancer from the oral cavity and oropharynx. *Eur J Gastroenterol Hepatol*. 2011; 23: 633-41.

[4] Johnson NW, Jayasekara P, Amarasinghe AA. Squamous cell carcinoma and precursor lesions of the oral cavity: epidemiology and aetiology. *Periodontol 2000*. 2011; 57: 19-37.

[5] Deshpande AM, Wong DT. Molecular mechanisms of head and neck cancer. *Expert Rev Anticancer Ther*. 2008; 8: 799-809.

[6] Nguyen LV, Vanner R, Dirks P, et al. Cancer stem cells: an evolving concept. *Nat Rev Cancer*. 2012; 12: 133-43.

[7] He Q, Liu Z, Zhao T, et al. Bmi1 drives stem-like properties and is associated with migration, invasion, and poor prognosis in tongue squamous cell carcinoma. *Int J Biol Sci*. 2015; 11: 1-10.

[8] Tamatani T, Takamaru N, Ohe G, et al. Expression of CD44, CD44v9, ABCG2, CD24, Bmi-1 and ALDH1 in stage I and II oral squamous cell carcinoma and their association with clinicopathological factors. *Oncol Lett*. 2018; 16: 1133-40.

[9] Locke M, Heywood M, Fawell S, et al. Retention of intrinsic stem cell hierarchies in carcinoma-derived cell lines. *Cancer Res*. 2005; 65: 8944-50.

[10] Clay MR, Tabor M, Owen JH, et al. Single-marker identification of head and neck squamous cell carcinoma cancer stem cells with aldehyde dehydrogenase. *Head Neck*. 2010; 32: 1195-201.

[11] Dalley AJ, Pitty LP, Major AG, et al. Expression of ABCG2 and Bmi-1 in oral potentially malignant lesions and oral squamous cell carcinoma. *Cancer Med*. 2014; 3: 273-83.

[12] Ortiz RC, Lopes NM, Amôr NG, et al. CD44 and ALDH1 immunoexpression as prognostic indicators of invasion and metastasis in oral squamous cell carcinoma. *J Oral Pathol Med*. 2018; 47: 740-47.

[13] Yu CC, Lo WL, Chen YW, et al. Bmi-1 Regulates Snail Expression and Promotes Metastasis Ability in Head and Neck Squamous Cancer-Derived ALDH1 Positive Cells. *J Oncol*. 2011; 2011.

[14] Thiery JP. Epithelial-mesenchymal transitions in development and pathologies. *Curr Opin Cell Biol*. 2003; 15: 740-6.

[15] Kalluri R, Weinberg RA. The basics of epithelial-mesenchymal transition. *J Clin Invest*. 2009; 119: 1420-8.

[16] Thiery JP, Acloque H, Huang RY, et al. Epithelial-mesenchymal transitions in development and disease. *Cell*. 2009; 139: 871-90.

[17] Zhou J, Tao D, Xu Q, et al. Expression of E-cadherin and vimentin in oral squamous cell carcinoma. *Int J Clin Exp Pathol*. 2015; 8: 3150-4.

[18] Biddle A, Liang X, Gammon L, et al. Cancer stem cells in squamous cell carcinoma switch between two distinct phenotypes that are preferentially migratory or proliferative. *Cancer Res*. 2011; 71: 5317-26.

[19] Mognetti B, Di Carlo F, Berta GN. Animal models in oral cancer research. *Oral Oncol*. 2006; 42: 448-60.

[20] Clarke MF, Dick JE, Dirks PB, et al. Cancer stem cells--perspectives on current status and future directions: AACR Workshop on cancer stem cells. *Cancer Res*. 2006; 66: 9339-44.

[21] Sano D, Myers JN. Xenograft models of head and neck cancers. *Head Neck Oncol*. 2009; 1: 32.

[22] Cekanova M, Rathore K. Animal models and therapeutic molecular targets of cancer: utility and limitations. *Drug Des Devel Ther*. 2014; 8: 1911-21.

[23] Gemenetzidis E, Gammon L, Biddle A, et al. Invasive oral cancer stem cells display resistance to ionising radiation. *Oncotarget*. 2015; 6: 43964-77.

[24] *World Health Organization Classification of Tumors. Pathology & Genetics. Head and Neck Tumors.*: IARC*Press*, 2005.

[25] Götz C, Bissinger O, Nobis C, et al. ALDH1 as a prognostic marker for lymph node metastasis in OSCC. *Biomed Rep*. 2018; 9: 284-90.

[26] Saluja TS, Ali M, Mishra P, et al. Prognostic Value of Cancer Stem Cell Markers in Potentially Malignant Disorders of Oral Mucosa: A Meta-analysis. *Cancer Epidemiol Biomarkers Prev*. 2019; 28: 144-53.

[27] Barbato L, Bocchetti M, Di Biase A, et al. Cancer Stem Cells and Targeting Strategies. *Cells*. 2019; 8.

[28] de Andrade NP, Rodrigues MF, Rodini CO, et al. Cancer stem cell, cytokeratins and epithelial to mesenchymal transition markers expression in oral squamous cell carcinoma derived from ortothopic xenoimplantation of CD44. *Pathol Res Pract*. 2017; 213: 235-44.

[29] Al-Hajj M, Wicha MS, Benito-Hernandez A, et al. Prospective identification of tumorigenic breast cancer cells. *Proc Natl Acad Sci U S A*. 2003; 100: 3983-8.

[30] Sen S, Carnelio S. Expression of epithelial cell adhesion molecule (EpCAM) in oral squamous cell carcinoma. *Histopathology*. 2016; 68: 897-904.

[31] Ahmed S, Jayan L, Dineshkumar T, et al. Oral squamous cell carcinoma under microscopic vision: A review of histological variants and its prognostic indicators. *SRM Journal of Research in Dental Sciences*. 2019; 10: 90-97.

[32] Thompson LDR. Squamous cell carcinoma variants of the head and neck. *MINI-SYMPOSIUM:HEADANDNECK PATHOLOGY*: Current Diagnostic Pathology, 2003; 384-96.

[33] Hu J, Mirshahidi S, Simental A, et al. Cancer stem cell self-renewal as a therapeutic target in human oral cancer. *Oncogene*. 2019; 38: 5440-56.

[34] Bansal N, Bartucci M, Yusuff S, et al. BMI-1 Targeting Interferes with Patient-Derived Tumor-Initiating Cell Survival and Tumor Growth in Prostate Cancer. *Clin Cancer Res*. 2016; 22: 6176-91.

[35] Feng JQ, Xu ZY, Shi LJ, et al. Expression of cancer stem cell markers ALDH1 and Bmi1 in oral erythroplakia and the risk of oral cancer. *J Oral Pathol Med*. 2013; 42: 148-53.

[36] Bittar RF, Ferraro HP, Ribas MH, et al. Predictive factors of occult neck metastasis in patients with oral squamous cell carcinoma. *Braz J Otorhinolaryngol*. 2016; 82: 543-7.

[37] Costa LC, Leite CF, Cardoso SV, et al. Expression of epithelial-mesenchymal transition markers at the invasive front of oral squamous cell carcinoma. *J Appl Oral Sci*. 2015; 23: 169-78.

[38] Danielsson F, Peterson MK, Caldeira Araújo H, et al. Vimentin Diversity in Health and Disease. *Cells*. 2018; 7.

[39] Irani S, Jafari B. Expression of vimentin and CD44 in mucoepidermoid carcinoma: A role in tumor growth. *Indian J Dent Res*. 2018; 29: 333-40.

[40] Yamashita N, Tokunaga E, Inoue Y, et al. Clinical significance of co-expression of E-cadherin and vimentin in invasive breast cancer. *Journal of Clinical Oncology*. 2015; 33: e22013-e13.

3 DISCUSSION

3 DISCUSSION

CSC have been subjected to intensive studies due to their capacities to propagate and support tumorigenesis. CSC biomarkers investigation has been widely used as a pathway to target these cells in attempt to identify OSCC high-risk cases to overcome cancer progression and improve therapeutic outcomes (GÖTZ; BISSINGER; NOBIS; WOLFF *et al.*, 2018; SALUJA; ALI; MISHRA; KUMAR *et al.*, 2019). The present study evaluated OSCC development *in vivo* and assessed the well-established CSC (CD44, ALDH1, and BMI1) and EMT (E-cadherin, Vimentin, and SNAIL) makers by means of IHC in OSCC-derived tumors in NOD/SCID mice. The aim was to evaluate the differential tumorigenic potential of CSC subpopulation as well as to determine whether human carcinomas dysplastic characteristics and immunolabeling pattern reflects upon xenografted tumors.

To study mechanisms of OSCC initiation and progression, injection of human OSCC cell lines in immunocompromised mice's tongue provides an organ-specific microenvironment, which contributes to interactions between cancer cells and the surrounding non-cancerous stroma (CEKANOVA; RATHORE, 2014; MOGNETTI; DI CARLO; BERTA, 2006). Our results revealed that both LUC4 Epi-CSC and EMT-CSC subpopulations were capable to form microscopic tumors *in vivo,* supporting the idea that $CD44^{+}$ cells own tumor-initiating ability, for that reason are CSC. Accordingly, researchers associated high tumorigenic potential with $CD44^{high}$ and $CD44^{high}$/ALDH+ cells, which were isolated from patient-derived primary HNSCC specimens and xenoimplanted into the tongue of NOD/SCID mice (CHINN; DARR; OWEN; BELLILE *et al.*, 2015). In a different study, SCC9 $CD44^{High}$ cells were more tumorigenic and capable to originate heterogeneous tumors when compared with $CD44^{Low}$ cells in an orthotopic mouse model of oral cancer (DE ANDRADE; RODRIGUES; RODINI; NUNES, 2017). In addition, we observed that Epi-CSC showed higher capacity to colonize the primary site of inoculation and to form larger tumors *in vivo* than EMT-CSC cells. Likewise, a study conducted with human breast cancer obtained similar results by injection $ESA^{+}CD44^{+}CD24^{-}$ cells into immunocompromised mice (AL-HAJJ; WICHA; BENITO-HERNANDEZ; MORRISON *et al.*, 2003). Significantly, ESA-positive OSCC are linked to the worst prognosis being related to tumor size, histological grade and survival (SEN; CARNELIO, 2016). That way, cancer cells positive to both CD44 and ESA molecules have great capacity to colonize and re-establish the original tumor heterogeneity in mouse model.

Our study also investigated whether xenografted tumors displayed histopathological similarities with human OSCC. Microscopically, OSCC is formed by neoplastic epithelial cells that display distinct stages of squamous differentiation (AHMED; JAYAN; DINESHKUMAR; RAMAN, 2019). Malignant cells exhibiting disordered growth, keratin pearls formation, altered nuclear-cytoplasmic ratio, nuclear chromatin irregularities and increased mitotic figures are the most common findings in OSCC (THOMPSON, 2003). Forty-nine days post-injection, tumors derived from both CSC subpopulations presented OSCC traits, such as*: islets* of tumor cells with keratin pearl formation, distinct nuclear pleomorphism, hyperchromasia, abnormal mitoses and multinucleated cells. These results suggest that xenograft-derived tumors, mostly Epi-CSC-derived tumors, resemble closely to architectural and cellular changes found in human OSCC.

Moreover, our results demonstrated that tumors generated by both CSC subpopulations conserved CD44 immunoexpression and exhibited similar cytoplasmatic expression of ALDH-1, indicating that tumor cells preserved their CSC phenotype. Besides that, we observed that BMI1 was higher stained in tumors derived from Epi-CSC than EMT-CSC. Notably, a study showed that BMI1 is highly expressed in OSCC CSC and its inhibition attenuates oral CSC self-renewal and tumor-initiating potential (HU; MIRSHAHIDI; SIMENTAL; LEE *et al.*, 2019). Furthermore, in a prostate cancer study, inhibition of BMI1 in patient-derived cells decreased colony formation *in vitro* and tumor initiation *in vivo (BANSAL; BARTUCCI; YUSUFF; DAVIS et al., 2016).* In a different study, HNSCC-ALDH1^{+} cells exhibited high levels of BMI1 and stemness properties were enhanced in HNSCC-ALDH1^{-} cells when BMI1 was overexpressed by SNAIL upregulation (YU; LO; CHEN; HUANG *et al.*, 2011). Similarly, we found a positive correlation between BMI1 and ALDH1 in Epi-CSC-derived tumors, suggesting that they might be valuable predictors for evaluating the risk of oral cancer.

Although the EMT-CSC were described as cells in EMT (BIDDLE; LIANG; GAMMON; FAZIL *et al.*, 2011), tumors derived from EMT-CSC stained for E-cadherin and SNAIL in a very similar intensity to Epi-CSC-derived tumors. Controversially, we also showed that Vimentin was more present in Epi-CSC-derived carcinomas. Vimentin has been reported as a component of mesenchymal cells, but it is also highly found in non-mesenchymal cells, like epithelial cells in EMT process (DANIELSSON; PETERSON; CALDEIRA ARAÚJO; LAUTENSCHLÄGER *et al.*, 2018), suggesting that Epi-CSC injected into the tongue of mice might be entering in the EMT program. We also identified upregulation of CD44 and Vimentin at the ITF and both markers were significantly correlated in Epi-CSC carcinomas. Accordingly,

in a mucoepidermoid carcinoma, cancer cells were positive for both Vimentin and CD44 at the ITF, establishing an association between these markers and cancer invasion (IRANI; JAFARI, 2018). We also showed a positive correlation between Vimentin and E-cadherin in Epi-CSC carcinomas. Interestingly, co-expression of Vimentin and E-cadherin is associated with the most aggressive phenotype and poor prognosis in breast cancer (YAMASHITA; TOKUNAGA; INOUE; TANAKA *et al.*, 2015). In the same way, Vimentin and E-cadherin positive expressions were linked to OSCC metastases (ZHOU; TAO; XU; GAO *et al.*, 2015). However, we were unable to detect cervical lymph node metastasis in order to precisely establish the association between these markers and invasion. Long-term protocols should be conducted to evaluate the ability of both CSC subpopulations to metastasize.

To conclude, in mouse-induced Epi-CSC tumors, CSC and EMT-related proteins expression mimicked strong similarity to human OSCC and have a contribution to elucidate CSCs behavior *in vivo*. Correlating CSC subpopulations with their corresponding tumors *in vivo* might highlight the role of different CSC phenotypes in OSCC development and progression. Further studies should be conducted in this field aiming the understanding of how they CSC subpopulations respond in commonly used therapeutics and development of techniques to overcome their resistance mechanisms. Regarding metastasis assessment, increasing experimental protocol time is advisable to evaluate the relationship between EMT-related proteins and lymph node metastases.

4 CONCLUSION

4 CONCLUSION

In conclusion, using the surface markers CD44 and ESA we isolated two different phenotypes of CSC from OSCC. Epi-CSC displayed high tumorigenic potential to form heterogeneous tumors into NOD/SCID mice 49 days-post inoculation. Moreover, these tumors reproduced histopathological and immunolabeling pattern similar to human OSCC suggesting that xenografting Epi-CSC into immunocompromised mice represent a trustworthy approach for future oral cancer research.

REFERENCES

REFERENCES

ABDOUH, M.; FACCHINO, S.; CHATOO, W.; BALASINGAM, V. *et al.* BMI1 sustains human glioblastoma multiforme stem cell renewal. **J Neurosci**, 29, n. 28, p. 8884-8896, Jul 2009.

AHMED, S.; JAYAN, L.; DINESHKUMAR, T.; RAMAN, S. Oral squamous cell carcinoma under microscopic vision: A review of histological variants and its prognostic indicators. **SRM Journal of Research in Dental Sciences**, 10, n. 2, p. 90-97, April 1, 2019 2019. Review Article.

AL-HAJJ, M.; WICHA, M. S.; BENITO-HERNANDEZ, A.; MORRISON, S. J. *et al.* Prospective identification of tumorigenic breast cancer cells. **Proc Natl Acad Sci U S A**, 100, n. 7, p. 3983-3988, Apr 2003.

BANSAL, N.; BARTUCCI, M.; YUSUFF, S.; DAVIS, S. *et al.* BMI-1 Targeting Interferes with Patient-Derived Tumor-Initiating Cell Survival and Tumor Growth in Prostate Cancer. **Clin Cancer Res**, 22, n. 24, p. 6176-6191, Dec 2016.

BIDDLE, A.; LIANG, X.; GAMMON, L.; FAZIL, B. *et al.* Cancer stem cells in squamous cell carcinoma switch between two distinct phenotypes that are preferentially migratory or proliferative. **Cancer Res**, 71, n. 15, p. 5317-5326, Aug 2011.

BONNET, D.; DICK, J. E. Human acute myeloid leukemia is organized as a hierarchy that originates from a primitive hematopoietic cell. **Nat Med**, 3, n. 7, p. 730-737, Jul 1997.

CEKANOVA, M.; RATHORE, K. Animal models and therapeutic molecular targets of cancer: utility and limitations. **Drug Des Devel Ther**, 8, p. 1911-1921, 2014.

CHINN, S. B.; DARR, O. A.; OWEN, J. H.; BELLILE, E. *et al.* Cancer stem cells: mediators of tumorigenesis and metastasis in head and neck squamous cell carcinoma. **Head Neck**, 37, n. 3, p. 317-326, Mar 2015.

CLAY, M. R.; TABOR, M.; OWEN, J. H.; CAREY, T. E. *et al.* Single-marker identification of head and neck squamous cell carcinoma cancer stem cells with aldehyde dehydrogenase. **Head Neck**, 32, n. 9, p. 1195-1201, Sep 2010.

CLEVERS, H. The cancer stem cell: premises, promises and challenges. **Nat Med**, 17, n. 3, p. 313-319, Mar 2011.

COSTA, L. C.; LEITE, C. F.; CARDOSO, S. V.; LOYOLA, A. M. *et al.* Expression of epithelial-mesenchymal transition markers at the invasive front of oral squamous cell carcinoma. **J Appl Oral Sci**, 23, n. 2, p. 169-178, 2015 Mar-Apr 2015.

DANIELSSON, F.; PETERSON, M. K.; CALDEIRA ARAÚJO, H.; LAUTENSCHLÄGER, F. *et al.* Vimentin Diversity in Health and Disease. **Cells**, 7, n. 10, Sep 2018.

DAWOOD, S.; AUSTIN, L.; CRISTOFANILLI, M. Cancer stem cells: implications for cancer therapy. **Oncology (Williston Park)**, 28, n. 12, p. 1101-1107, 1110, Dec 2014.

DE ANDRADE, N. P.; RODRIGUES, M. F.; RODINI, C. O.; NUNES, F. D. Cancer stem cell, cytokeratins and epithelial to mesenchymal transition markers expression in oral squamous cell carcinoma derived from ortothopic xenoimplantation of CD44. **Pathol Res Pract**, 213, n. 3, p. 235-244, Mar 2017.

EGUSA, H.; SONOYAMA, W.; NISHIMURA, M.; ATSUTA, I. *et al.* Stem cells in dentistry--part I: stem cell sources. **J Prosthodont Res**, 56, n. 3, p. 151-165, Jul 2012.

ERAMO, A.; LOTTI, F.; SETTE, G.; PILOZZI, E. *et al.* Identification and expansion of the tumorigenic lung cancer stem cell population. **Cell Death Differ**, 15, n. 3, p. 504-514, Mar 2008.

FEDELE, M.; CERCHIA, L.; CHIAPPETTA, G. The Epithelial-to-Mesenchymal Transition in Breast Cancer: Focus on Basal-Like Carcinomas. **Cancers (Basel)**, 9, n. 10, Sep 2017.

GINESTIER, C.; HUR, M. H.; CHARAFE-JAUFFRET, E.; MONVILLE, F. *et al.* ALDH1 is a marker of normal and malignant human mammary stem cells and a predictor of poor clinical outcome. **Cell Stem Cell**, 1, n. 5, p. 555-567, Nov 2007.

GÖTZ, C.; BISSINGER, O.; NOBIS, C.; WOLFF, K. D. *et al.* ALDH1 as a prognostic marker for lymph node metastasis in OSCC. **Biomed Rep**, 9, n. 4, p. 284-290, Oct 2018.

HANNEN, E. J.; VAN DER LAAK, J. A.; MANNI, J. J.; PAHLPLATZ, M. M. *et al.* Improved prediction of metastasis in tongue carcinomas, combining vascular and nuclear tumor parameters. **Cancer**, 92, n. 7, p. 1881-1887, Oct 2001.

HERREROS-VILLANUEVA, M.; ZHANG, J. S.; KOENIG, A.; ABEL, E. V. *et al.* SOX2 promotes dedifferentiation and imparts stem cell-like features to pancreatic cancer cells. **Oncogenesis**, 2, p. e61, Aug 2013.

HU, J.; MIRSHAHIDI, S.; SIMENTAL, A.; LEE, S. C. *et al.* Cancer stem cell self-renewal as a therapeutic target in human oral cancer. **Oncogene**, 38, n. 27, p. 5440-5456, 07 2019.

IRANI, S.; JAFARI, B. Expression of vimentin and CD44 in mucoepidermoid carcinoma: A role in tumor growth. **Indian J Dent Res**, 29, n. 3, p. 333-340, 2018 May-Jun 2018.

JÄRVINEN, A. K.; AUTIO, R.; KILPINEN, S.; SAARELA, M. *et al.* High-resolution copy number and gene expression microarray analyses of head and neck squamous cell carcinoma cell lines of tongue and larynx. **Genes Chromosomes Cancer**, 47, n. 6, p. 500-509, Jun 2008.

KALLURI, R.; WEINBERG, R. A. The basics of epithelial-mesenchymal transition. **J Clin Invest**, 119, n. 6, p. 1420-1428, Jun 2009.

KANOJIA, D.; VAIDYA, M. M. 4-nitroquinoline-1-oxide induced experimental oral carcinogenesis. **Oral Oncol**, 42, n. 7, p. 655-667, Aug 2006.

KOREN, E.; FUCHS, Y. The bad seed: Cancer stem cells in tumor development and resistance. **Drug Resist Updat**, 28, p. 1-12, 09 2016.

KOSUNEN, A.; PIRINEN, R.; ROPPONEN, K.; PUKKILA, M. *et al.* CD44 expression and its relationship with MMP-9, clinicopathological factors and survival in oral squamous cell carcinoma. **Oral Oncol**, 43, n. 1, p. 51-59, Jan 2007.

LEMISCHKA, I. R. Stem cell biology: a view toward the future. **Ann N Y Acad Sci**, 1044, p. 132-138, Jun 2005.

LIU, P. F.; KANG, B. H.; WU, Y. M.; SUN, J. H. *et al.* Vimentin is a potential prognostic factor for tongue squamous cell carcinoma among five epithelial-mesenchymal transition-related proteins. **PLoS One**, 12, n. 6, p. e0178581, 2017.

LOCKE, M.; HEYWOOD, M.; FAWELL, S.; MACKENZIE, I. C. Retention of intrinsic stem cell hierarchies in carcinoma-derived cell lines. **Cancer Res**, 65, n. 19, p. 8944-8950, Oct 2005.

LUKACS, R. U.; GOLDSTEIN, A. S.; LAWSON, D. A.; CHENG, D. *et al.* Isolation, cultivation and characterization of adult murine prostate stem cells. **Nat Protoc**, 5, n. 4, p. 702-713, Apr 2010.

MAAYAH, Z. H.; GHEBEH, H.; ALHAIDER, A. A.; EL-KADI, A. O. *et al.* Metformin inhibits 7,12-dimethylbenz[a]anthracene-induced breast carcinogenesis and adduct formation in human breast cells by inhibiting the cytochrome P4501A1/aryl hydrocarbon receptor signaling pathway. **Toxicol Appl Pharmacol**, 284, n. 2, p. 217-226, Apr 2015.

MEACHAM, C. E.; MORRISON, S. J. Tumour heterogeneity and cancer cell plasticity. **Nature**, 501, n. 7467, p. 328-337, Sep 2013.

MOGNETTI, B.; DI CARLO, F.; BERTA, G. N. Animal models in oral cancer research. **Oral Oncol**, 42, n. 5, p. 448-460, May 2006.

O'BRIEN, C. A.; POLLETT, A.; GALLINGER, S.; DICK, J. E. A human colon cancer cell capable of initiating tumour growth in immunodeficient mice. **Nature**, 445, n. 7123, p. 106-110, Jan 2007.

ORTIZ, R. C.; LOPES, N. M.; AMÔR, N. G.; PONCE, J. B. *et al.* CD44 and ALDH1 immunoexpression as prognostic indicators of invasion and metastasis in oral squamous cell carcinoma. **J Oral Pathol Med**, 47, n. 8, p. 740-747, Sep 2018.

PARSANA, P.; AMEND, S. R.; HERNANDEZ, J.; PIENTA, K. J. *et al.* Identifying global expression patterns and key regulators in epithelial to mesenchymal transition through multi-study integration. **BMC Cancer**, 17, n. 1, p. 447, Jun 2017.

PATRAWALA, L.; CALHOUN, T.; SCHNEIDER-BROUSSARD, R.; LI, H. *et al.* Highly purified CD44+ prostate cancer cells from xenograft human tumors are enriched in tumorigenic and metastatic progenitor cells. **Oncogene**, 25, n. 12, p. 1696-1708, Mar 2006.

PETRICK, J. L.; WYSS, A. B.; BUTLER, A. M.; CUMMINGS, C. *et al.* Prevalence of human papillomavirus among oesophageal squamous cell carcinoma cases: systematic review and meta-analysis. **Br J Cancer**, 110, n. 9, p. 2369-2377, Apr 2014.

PIFFKÒ, J.; BÀNKFALVI, A.; OFNER, D.; BRYNE, M. *et al.* Prognostic value of histobiological factors (malignancy grading and AgNOR content) assessed at the invasive tumour front of oral squamous cell carcinomas. **Br J Cancer**, 75, n. 10, p. 1543-1546, 1997.

PRINCE, M. E.; SIVANANDAN, R.; KACZOROWSKI, A.; WOLF, G. T. *et al.* Identification of a subpopulation of cells with cancer stem cell properties in head and neck squamous cell carcinoma. **Proc Natl Acad Sci U S A**, 104, n. 3, p. 973-978, Jan 2007.

RAJU, B.; IBRAHIM, S. O. Pathophysiology of oral cancer in experimental animal models: a review with focus on the role of sympathetic nerves. **J Oral Pathol Med**, 40, n. 1, p. 1-9, Jan 2011.

REYA, T.; MORRISON, S. J.; CLARKE, M. F.; WEISSMAN, I. L. Stem cells, cancer, and cancer stem cells. **Nature**, 414, n. 6859, p. 105-111, Nov 2001.

SALUJA, T. S.; ALI, M.; MISHRA, P.; KUMAR, V. *et al.* Prognostic Value of Cancer Stem Cell Markers in Potentially Malignant Disorders of Oral Mucosa: A Meta-analysis. **Cancer Epidemiol Biomarkers Prev**, 28, n. 1, p. 144-153, 01 2019.

SCHATTON, T.; FRANK, M. H. The in vitro spheroid melanoma cell culture assay: cues on tumor initiation? **J Invest Dermatol**, 130, n. 7, p. 1769-1771, Jul 2010.

SEN, S.; CARNELIO, S. Expression of epithelial cell adhesion molecule (EpCAM) in oral squamous cell carcinoma. **Histopathology**, 68, n. 6, p. 897-904, May 2016.

SHIGDAR, S.; LI, Y.; BHATTACHARYA, S.; O'CONNOR, M. *et al.* Inflammation and cancer stem cells. **Cancer Lett**, 345, n. 2, p. 271-278, Apr 2014.

SINGH, S. K.; CLARKE, I. D.; TERASAKI, M.; BONN, V. E. *et al.* Identification of a cancer stem cell in human brain tumors. **Cancer Res**, 63, n. 18, p. 5821-5828, Sep 2003.

SMITH, A.; TEKNOS, T. N.; PAN, Q. Epithelial to mesenchymal transition in head and neck squamous cell carcinoma. **Oral Oncol**, 49, n. 4, p. 287-292, Apr 2013.

SZANISZLO, P.; FENNEWALD, S. M.; QIU, S.; KANTARA, C. *et al.* Temporal characterization of lymphatic metastasis in an orthotopic mouse model of oral cancer. **Head Neck**, 36, n. 11, p. 1638-1647, Nov 2014.

THIERAUF, J.; VEIT, J. A.; HESS, J. Epithelial-to-Mesenchymal Transition in the Pathogenesis and Therapy of Head and Neck Cancer. **Cancers (Basel)**, 9, n. 7, Jul 2017.

THIERY, J. P. Epithelial-mesenchymal transitions in development and pathologies. **Curr Opin Cell Biol**, 15, n. 6, p. 740-746, Dec 2003.

THOMPSON, L. D. R. Squamous cell carcinoma variants of the head and neck. MINI-SYMPOSIUM:HEADANDNECK PATHOLOGY. Current Diagnostic Pathology. 9**:** 384-396 p. 2003.

VALENT, P.; BONNET, D.; DE MARIA, R.; LAPIDOT, T. *et al.* Cancer stem cell definitions and terminology: the devil is in the details. **Nat Rev Cancer**, 12, n. 11, p. 767-775, 11 2012.

VERED, M.; YAROM, N.; DAYAN, D. 4NQO oral carcinogenesis: animal models, molecular markers and future expectations. **Oral Oncol**, 41, n. 4, p. 337-339, Apr 2005.

WACLAW, B.; BOZIC, I.; PITTMAN, M. E.; HRUBAN, R. H. *et al.* A spatial model predicts that dispersal and cell turnover limit intratumour heterogeneity. **Nature**, 525, n. 7568, p. 261-264, Sep 2015.

YAMASHITA, N.; TOKUNAGA, E.; INOUE, Y.; TANAKA, K. *et al.* Clinical significance of co-expression of E-cadherin and vimentin in invasive breast cancer. **Journal of Clinical Oncology**, 33, n. 15_suppl, p. e22013-e22013, 2015.

YANG, M. H.; CHANG, S. Y.; CHIOU, S. H.; LIU, C. J. *et al.* Overexpression of NBS1 induces epithelial-mesenchymal transition and co-expression of NBS1 and Snail predicts metastasis of head and neck cancer. **Oncogene**, 26, n. 10, p. 1459-1467, Mar 2007.

YU, C. C.; LO, W. L.; CHEN, Y. W.; HUANG, P. I. *et al.* Bmi-1 Regulates Snail Expression and Promotes Metastasis Ability in Head and Neck Squamous Cancer-Derived ALDH1 Positive Cells. **J Oncol**, 2011, 2011.

ZHOU, J.; TAO, D.; XU, Q.; GAO, Z. *et al.* Expression of E-cadherin and vimentin in oral squamous cell carcinoma. **Int J Clin Exp Pathol**, 8, n. 3, p. 3150-3154, 2015.

ANNEX

Universidade de São Paulo
Faculdade de Odontologia de Bauru

Comissão de Ética no Ensino e Pesquisa em Animais

CEEPA-Proc. Nº 002/2017.

Bauru, 5 de maio de 2017.

Senhora Professora,

Informamos que Projeto de Pesquisa denominado ***"Caracterização da Relação Funcional entre Macrófagos, Fenótipo Célula-Tronco de Câncer e Fenômeno de Transição Epitélio-Mesenquimal no Carcinoma Epidermóide de Boca"*** tendo Vossa Senhoria como Pesquisador Responsável, que envolve a utilização de animais (roedores), para fins de pesquisa científica, encontra-se de acordo com os preceitos da Lei nº 11.794, de 8 de outubro de 2008, do Decreto nº 6.899, de 15 de julho de 2009, e com as normas editadas pelo Conselho Nacional de Controle da Experimentação Animal (CONCEA), foi analisado e considerado APROVADO em reunião ordinária da Comissão de Ética no Ensino e Pesquisa em Animais (CEEPA), realizada nesta data.

Vigência do projeto:	*Maio/2017 a Maio/2020*
Espécie/Linhagem:	*Camundongos imunodeficientes NOD/SCID*
Nº de animais:	*300*
Peso/Idade	*20g/6-8 semanas*
Sexo:	*Machos e fêmeas*
Origem:	*Centro de Bioterismo da Faculdade de Medicina da USP*

Esta CEEPA solicita que ao final da pesquisa seja enviado um Relatório com os resultados obtidos para análise ética e emissão de parecer final, o qual poderá ser utilizado para fins de publicação científica.

Atenciosamente,

Profª Drª Ana Paula Campanelli

Presidente da Comissão de Ética no Ensino e Pesquisa em Animais

Profa. Dra. Camila de Oliveira Rodini Pegoraro
Docente do Departamento de Ciências Biológicas

Al. Dr. Octávio Pinheiro Brisolla, 9-75 – Bauru-SP – CEP 17012-901 – C.P. 73
e-mail: ceepa@fob.usp.br – Fone/FAX (0xx14) 3235-8356
http://www.fob.usp.br